Title: Characterization of multiple *SPS* knockout mutants reveals redundant functions of the four Arabidopsis sucrose phosphate synthase isoforms in plant viability, and strongly indicates that enhanced respiration and accelerated starch turnover can alleviate the blockage of sucrose biosynthesis

Authors: Abdellatif Bahaji[¶1], Edurne Baroja-Fernández[¶1], Adriana Ricarte-Bermejo[1], Ángela María Sánchez-López[1], Francisco José Muñoz[1], Jose M. Romero[2], María Teresa Ruiz[2], Marouane Baslam[1], Goizeder Almagro[1], María Teresa Sesma[1] and Javier Pozueta-Romero*[1]

Affiliations: (1) Instituto de Agrobiotecnología (CSIC/UPNA/Gobierno de Navarra). Iruñako etorbidea 123, 31192 Mutiloabeti, Nafarroa, Spain. (2) Instituto de Bioquímica Vegetal y Fotosíntesis. Universidad de Sevilla-CSIC. Avenida Américo Vespucio 49. Isla de la Cartuja, 41092, Sevilla, Spain.

***Corresponding author:** Javier Pozueta Romero.

Address: Instituto de Agrobiotecnología. Iruñako etorbidea 123, 31192 Mutiloabeti, Nafarroa, Spain. E-mail: javier.pozueta@unavarra.es. Phone: (34) 948168009. FAX: (34) 948232191

[¶]A.B. and E.B.-F. have equally contributed to this work.

Abbreviations: A_n, net photosynthetic CO_2 fixation rate; ADPG, ADP-glucose; AGP, ADPG pyrophosphorylase; Ci, intercellular CO_2 concentrations; CL, continuous light; DAG, days after germination; $F1,6P_2$, fructose-1,6-bisphosphate; F6P, fructose-6-phosphate; G1P, glucose-1-phosphate; G6P, glucose-6-phosphate; G6PDH, G6P dehydrogenase; g_s, stomatal conductance; G3PDH, glyceraldehyde-3-phosphate dehydrogenase; HK, hexokinase; IDH, isocitrate dehydrogenase; MDH, malate dehydrogenase; OPPP, oxidative pentose phosphate pathway; PEP, phospho-enol-pyruvate; 3-PGA, 3-phosphoglycerate; PGI, phosphoglucose isomerase; 6PGDH, 6-phosphogluconate dehydrogenase; PGM, phosphoglucomutase; Pi, inorganic orthophosphate; PK, pyruvate kinase; PPase, alkaline pyrophosphatase; S6P, sucrose-6-phosphate; SDH, succinate dehydrogenase; SPP, sucrose-phosphate phosphatase; SPS,

sucrose-phosphate synthase; SS, starch synthase; SuSy, sucrose synthase; TCA, tricarboxylic acid cycle; TPT, triose-phosphate/phosphate translocator; U, unit of enzyme activity; UDPG, UDP-glucose; UGP, UDPG pyrophosphorylase; WT, wild type

ABSTRACT

We characterized multiple knock-out mutants of the four Arabidopsis sucrose phosphate synthase (SPSA1, SPSA2, SPSB and SPSC) isoforms. Despite their reduced SPS activity, *spsa1/spsa2, spsa1/spsb, spsa2/spsb, spsa2/spsc, spsb/spsc*, *spsa1/spsa2/spsb* and *spsa2/spsb/spsc* mutants displayed wild type (WT) vegetative and reproductive morphology, and showed WT photosynthetic capacity and respiration. In contrast, growth of rosettes, flowers and siliques of the *spsa1/spsc* and *spsa1/spsa2/spsc* mutants was reduced compared with WT plants. Furthermore, these plants displayed a high dark respiration phenotype. *spsa1/spsb/spsc* and *spsa1/spsa2/spsb/spsc* seeds poorly germinated and produced aberrant and sterile plants. Leaves of all viable *sps* mutants, except *spsa1/spsc* and *spsa1/spsa2/spsc,* accumulated WT levels of nonstructural carbohydrates. *spsa1/spsc* leaves possessed high levels of metabolic intermediates and activities of enzymes of the glycolytic and tricarboxylic acid cycle pathways, and accumulated high levels of metabolic intermediates of the nocturnal starch-to-sucrose conversion process, even under continuous light conditions. Results presented in this work show that SPS is essential for plant viability, reveal redundant functions of the four SPS isoforms in processes that are important for plant growth and nonstructural carbohydrate metabolism, and strongly indicate that accelerated starch turnover and enhanced respiration can alleviate the blockage of sucrose biosynthesis in *spsa1/spsc* leaves.

Keywords: Carbohydrate metabolism, development, functional interaction, genetic redundancy, growth, sucrose

1. Introduction

In the majority of higher plants sucrose is the main end-product of photosynthesis. It serves as the mobile form of photoassimilate that is transported from leaves to sink organs. This disaccharide plays a major role in growth, and also acts as a signaling molecule in the control of the expression of genes involved in multiple processes such as central carbon and nitrogen metabolisms [1], storage of proteins [2], cell cycle and differentiation [3], flowering [4] and seed development [5]. During the day, photosynthetically fixed carbon is either retained within the chloroplast of leaf mesophyll cells to fuel the synthesis of transitory starch, or exported to the cytosol as triose phosphates by means of the triose-phosphate/phosphate translocator (TPT) to be converted into activated forms of hexoses and sucrose (**Fig. S1A**). Sucrose is synthesized by the action of two enzymes: sucrose-phosphate synthase (SPS, which catalyzes the conversion of fructose-6-phosphate (F6P) and UDP-glucose (UDPG) into sucrose-6-phosphate (S6P)), and sucrose-phosphate phosphatase (SPP, which hydrolyzes S6P to produce sucrose) (**Fig. S1A**). During the night, starch is mobilized to produce maltose that is transported to the cytosol by means of the MEX1 translocator (**Fig. S1B**). Once in the cytosol maltose is converted into heteroglycans, glucose-1-P (G1P), UDPG, S6P and sucrose by the stepwise reactions of the cytosolic disproportionating enzyme DPE2, glucan phosphorylase PHS2, UDPG pyrophosphorylase (UGP), SPS and SPP [6-8] (**Fig. S1B**). Glucose, another starch breakdown product, can be transported to the cytosol by means of the pGlcT transporter [9]. Once in the cytosol, glucose can be converted into glucose-6-P (G6P), G1P, UDPG, S6P and sucrose by the stepwise reactions of hexokinase (HK), phosphoglucomutase (PGM), UGP, SPS and SPP [9] (**Fig. S1B**).

SPS is a key control point of carbon flux into sucrose that is regulated by a hierarchy of mechanisms including posttranslational modification via protein phosphorylation, activation by G6P and inhibition by inorganic orthophosphate (Pi) [10,11], and transcriptional regulation of *SPS* gene expression [12,13]. SPS isoforms in the many plant species examined to date are encoded by a small *SPS* multigene family. Studies of the predicted amino acid sequences and gene structure have shown that the *Arabidopsis* SPS family consists of four *SPS* genes, referred to as *AtSPSA1* (At5g20280), *AtSPSA2* (At5g11110), *AtSPSB* (At1g04920) and *AtSPSC* (At4g10120) [14,15]. Genome-

wide expression analyses (https://www.geneinvestigator.ethz.ch) and comparative studies of *SPS* gene expression in *Arabidopsis* [14,15] provided evidence for distinct, but partially overlapping spatial and temporal expression patterns for the four *SPS* genes. Metabolic studies of an *spsa1/spsc* double knockout *Arabidopsis* mutant revealed effects on growth and leaf nonstructural carbohydrate metabolism in this mutant [15]. Thus *spsa1/spsc* plants cultured under 8 h light/16 h dark photoregime displayed a dwarf phenotype. Also, these plants accumulated low levels of sucrose and moderately high levels of both starch and maltose when compared with wild type (WT) plants, strongly indicating that SPSA1 and SPSC have overlapping functions in aspects related with growth and leaf nonstructural carbohydrate metabolism. According to Volkert et al. [15], the increase in starch was probably not due to an increased partitioning of carbon into starch, but was rather caused by an impaired starch mobilization during the night due to impairment in downstream metabolization of maltose.

Mutants impaired in TPT and cytosolic fructose 1,6-bisphosphatase display a nearly WT growth phenotype [16-19], strongly indicating the operation in these mutants of mechanism(s) of diurnal sucrose biosynthesis additional/alternative to that illustrated in **Fig. S1A,** and showing that TPT and cytosolic fructose 1,6-bisphosphatase are not essential for plant viability. While SPS catalyzes an undoubtedly crucial step in sucrose biosynthesis, the challenge still remains to determine if SPS is an essential function for plant viability and if, in addition to the functional overlapping occurring between SPSA1 and SPSC *in planta*, there are other functional interactions between the four SPS isoforms. Towards the end of exploring possible interactions between the four SPS isoforms *in planta*, and between sucrose biosynthesis and other metabolic pathways when SPS-mediated sucrose production is limited, in this work we conducted a comprehensive study of different multiple *SPS* knock-out mutants. Results presented in this work show that, in Arabidopsis, (a) SPS is essential for plant viability, implying that sucrose is mainly synthesized through the SPS-SPP pathway and (b) the four SPS isoforms are functionally redundant in processes that are important for plant growth, vegetative and reproductive development, and nonstructural carbohydrate metabolism. Furthermore, the results provide strong evidence supporting the occurrence in illuminated *spsa1/spsc* leaves of mechanisms alleviating the blockage of the starch-to-S6P conversion process

such as accelerated starch turnover, and channeling of starch breakdown products towards the glycolytic, oxidative pentose phosphate (OPP) and tricarboxylic acid cycle (TCA) pathways.

2. Materials and methods

2.1. Plants, growth conditions and sampling

Unless otherwise indicated WT *Arabidopsis thaliana* L. (Heynh) ecotype Columbia and T-DNA insertion lines in this background were cultured in soil in growth chambers under the indicated photoperiod conditions (light intensity of 90 µmol photons s^{-1} m^{-2}) (22ºC during the light period and 18ºC during the dark period). Harvested source leaves were immediately freeze-clamped and ground to a fine powder in liquid nitrogen with a pestle and mortar.

2.2. Production of multiple T-DNA knock-out lines

The T-DNA insertion mutants *spsa1* (SALK_119162), *spsa2* (SALK_064922), *spsb* (GABI_368F01) and *spsc* (SAIL_31_H05) were obtained from the European *Arabidopsis* Stock Center (NASC) (**Fig. S2**)**.** The T-DNA insertion in *spsa1* mutant is in the third intron, whereas the T-DNA insertions in *spsa2, spsb* and *spsc* are in the fifth, ninth and fifth exon of *SPSA2, SPSB* and *SPSC,* respectively (**Fig. S2**). By crossing these mutants, self-pollinating the resulting heterozygous mutants, and PCR screening for homozygous progeny using the oligonucleotide primers listed in **Table S2** we produced the *spsa1/spsa2, spsa1/spsb, spsa1/spsc, spsa2/spsb, spsa2/spsc, spsb/spsc*, *spsa1/spsb/spsc, spsa1/spsa2/spsb, spsa1/spsa2/spsc, spsa2/spsb/spsc*, and *spsa1/spsa2/spsb/spsc* mutants (**Table S1, Fig. S3**).

The knock-out status of the T-DNA mutants was confirmed by RT-PCR for *SPS* transcripts using specific primers that spanned the T-DNA insert site of each gene (**Table S3**). To this end, total RNA was extracted from leaves using the trizol method according to the manufacturer´s procedure (Invitrogen). RNA was treated with RNAase free DNAase (Takara). RT-PCR was conducted with SuperScript III one-step RT-PCR with Platinum *Taq* DNA polymerase kit (12574-018; Invitrogen) using 100 ng of RNA and the *SPSA1, SPSA2, SPSB* and *SPSC* specific primers listed in **Table S3**. 18S RNA was used

as the positive control. PCR products were separated on 1% (w/v) agarose gels containing ethidium bromide and visualized by ultraviolet light. *SPSA1, SPSA2, SPSB* and *SPSC* PCR products were detected in WT plants, but were undetectable in *spsa1, spsa2, spsb* and *spsc* mutants, respectively (**Fig. S4)**.

2.3. Enzyme assays

One g of the frozen powder (see above) was resuspended at 4ºC in 3 mL of 100 mM HEPES (pH 7.5), 2 mM EDTA, 2 mM dithiothreitol, 1 mM PMSF and 10 mL/L protease inhibitor cocktail (Sigma P9599), and centrifuged at 14,000 x g for 20 min. The supernatant was desalted by ultrafiltration on Vivaspin 500 centrifugal concentrator (Sartorius, Ref. VS0102) and the protein extract thus obtained was assayed for enzymatic activities. ADP-glucose (ADPG) pyrophosphorylase (AGP) and UGP activities were measured following the two-step assay method described in [20]. Phosphoglucose isomerase (PGI) and sucrose synthase (SuSy) activities were measured as described in [21] and [22], respectively. PGM and amylolytic activities were assayed as described in [23] and [24], respectively. Acid and alkaline invertases were measured as described in [25]. HK activity was assayed as described in [26]. Alkaline pyrophosphatase (PPase) and SPS were measured as described in [27]. Starch synthase (SS) activity was measured as described in [28]. Fructose-1,6-bisphosphate ($F1,6P_2$) aldolase, glyceraldehyde-3-phosphate dehydrogenase (G3PDH), 3-phosphoglycerate (3PGA) kinase and pyruvate kinase (PK) were measured as described in [29]. G6P dehydrogenase (G6PDH), 6-phosphogluconate dehydrogenase (6PGDH) and isocitrate dehydrogenase (IDH) were measured as described in [30]. Malate dehydrogenase (MDH) and succinate dehydrogenase (SDH) were measured as described in [31] and [32], respectively. One unit (U) is defined as the amount of enzyme that catalyzes the production of 1 µmol of product per min.

2.4. Non-reducing western blot analyses of AGP

For non-reducing western blots of AGP, 50 mg of the homogenized frozen material (see above) was extracted in cold 16% (w/v) trichloroacetic acid in diethyl ether, mixed, and stored at –20ºC for at least 2 h as described in [20]. The pellet was collected by

centrifugation at 10,000 x g for 5 min at 4ºC, washed 3 times with ice-cold acetone, dried briefly under vacuum, and resuspended in 1x Laemmli sample buffer containing no reductant. Protein samples were separated on 10% SDS-PAGE, transferred to nitrocellulose filters, and immunodecorated by using antisera raised against maize AGP as primary antibody [20], and a goat anti-rabbit IgG alkaline phosphatase conjugate (Sigma) as secondary antibody.

2.5. Native gel assay for PGM activity

PGM zymograms were performed essentially as described in [23]. Protein extracts (see above) of both WT and *spsa1/spsc* leaves were loaded onto a 7.5% (w/v) polyacrylamide gel. After electrophoresis gels were stained by incubating in darkness at room temperature with 0.1 M Tris-HCl (pH 8.0), 5 mM G1P, 1 mM NAD^+, 4 mM $MgCl_2$, 0.2 mM methylthiazolyldiphenyl-tetrazolium bromide (Sigma M5655) and 0.25 mM phenazine methosulfate (Sigma P9625) and 1 U/mL of G6PDH from *Leuconostoc mesenteroides* (Sigma G8404).

2.6. Analytical procedures

ADPG content was measured by HPLC-MS/MS as described in [33]. 3PGA was determined as described in [34]. For measurement of sucrose, glucose, maltose and fructose, a 0.1 g aliquot of the frozen leaf powder (see above) was resuspended in 1 mL of 90% ethanol, left at 70ºC for 90 min and centrifuged at 13,000 x g for 10 min. For measurement of G6P, F6P, F1,6P_2, S6P, UDPG and G1P 0.1 g aliquot of the frozen leaf powder was resuspended in 1 mL of 1 M $HClO_4$, left at 4ºC for 2 h and centrifuged at 10,000 x g for 5 min. The supernatant was neutralized with K_2CO_3 and centrifuged at 10,000 x g. Sucrose, glucose, fructose, maltose, F6P, F1,6P_2, G6P, S6P and G1P from the above supernatants were determined by HPLC with pulsed amperometric detection on a DX-500 Dionex system by gradient separation with a CarboPac 10 column according to the application method suggested by the supplier (100 mM NaOH/100 mM sodium acetate to 100 mM NaOH/500 mM sodium acetate in 40 min). UDPG was measured as described in [35] by HPLC on a system obtained from Waters Associates fitted with a Partisil-10-SAX column. Starch was measured by using an amyloglucosydase–based test

kit (Boehringer Mannheim, Germany). Oxaloacetate, pyruvate, phospho-enol-pyruvate (PEP) and isocitrate were determined as described in [36]. Recovery experiments were carried out by the addition of known amounts of metabolites standards to the frozen tissue slurry immediately after addition of extraction solutions. The difference in the measured amounts between the samples with and without added standards was used as an estimate of the percentage of recovery. All data were corrected for loss during extraction.

2.7. Iodine staining and microscopic localization of starch granules

Leaves harvested at the end of the light period were fixed by immersion into 3.7% formaldehyde in phosphate buffer. Leaf pigments were then removed in 96% ethanol. Re-hydrated samples were stained in iodine solution (KI 2% (w/v) I_2 1% (w/v)) for 30 min, rinsed briefly in deionized water and photographed. Samples for sectioning were immersed in cryoprotective medium OCT (Tissue-Tec, USA) and frozen at -50ºC. Cryosections of 10 µm thick were obtained in AS620 Cryotome (Shandon, England). After thawing, sections were stained in iodine solution for 2 min at room temperature, mounted to microscope slides and observed using a stereomicroscope Olympus MVX10 (Japan). Microphotographs were captured with video camera DP72 (Olympus, Japan) and Cell D software (Olympus, Japan).

2.8. Gas exchange determinations

Fully expanded apical leaves were enclosed in a LCipro portable photosynthesis system (ADC BioScientfic Ltd., Hoddesdon, Herts). Gas exchange parameters including net photosynthetic CO_2 fixation rate (A_n), stomatal conductance (g_s) and intercellular CO_2 concentrations (Ci) were measured at 25ºC with photosynthetic photon flux densities of 90 and 350 µmol m^{-2} s^{-1} and CO_2 concentration of 450 µmol mol^{-1}. A_n was calculated using equations developed in [37]. g_s values were determined as described in [38]. The rate of mitochondrial respiration in the dark was determined by measuring the rate of CO_2 evolution in the dark.

2.9. Statistical analysis

The data presented are the means of three independent experiments, with 3-5 replicates

for each experiment (means ± SE). The significance of differences between the control and the different *sps* mutants was statistically evaluated with Student´s t-test using the SPSS software. Differences were considered significant at a probability level of $P<0.05$.

3. Results

3.1. Phenotypic characterization of double, triple and quadruple AtSPS knockout mutants

We produced and characterized *spsa1/spsa2, spsa1/spsb, spsa1/spsc, spsa2/spsb, spsa2/spsc* and *spsb/spsc* double knock-out mutants, the *spsa1/spsb/spsc, spsa1/spsa2/spsb, spsa1/spsa2/spsc* and *spsa2/spsb/spsc* triple knock-out mutants, and the *spsa1/spsa2/spsb/spsc* quadruple knock-out mutant (**Fig. S3, Table S1**).

As shown in **Fig. 1A,B**, soil-grown *spsa1/spsa2, spsa1/spsb, spsa2/spsb, spsa2/spsc* and *spsb/spsc* double mutants grew at the same rate as WT plants, and displayed WT vegetative morphology. Furthermore, these mutants produced flowers and siliques displaying WT phenotype and fertile seeds (not shown). Noteworthy, the *spsa2/spsb/spsc* and the *spsa1/spsa2/spsb* triple mutants grew at the same rate as WT plants, displayed WT vegetative morphology (**Fig. 1A,B**), and produced flowers and siliques displaying WT phenotype (**Fig. 1C**), showing that SPSA1 expression in the total absence of SPSA2+SPSB+SPSC expression, and SPSC expression in the total absence of SPSA1+SPSA2+SPSB expression guarantee normal seed development, germination and subsequent development of the plant.

Growth of *spsa1/spsc* rosettes was reduced when compared with WT plants (**Fig. 1**), which is consistent with Volkert et al. [15]. This phenotype could be reverted to WT when plants were cultured in MS supplemented with sucrose (**Fig. S5**). Furthermore, *spsa1/spsc* flowers and siliques were small when compared with those of WT plants (**Fig. 1C**). Moreover, this mutant produced few seeds when compared with WT plants (not shown), the overall data thus strongly indicating that SPSA1 and SPSC play overlapping functions in processes that are important for both vegetative and reproductive growth. The *spsa1/spsa2/spsc* mutant was viable although its vegetative and reproductive growth was reduced when compared with that of *spsa1/spsc* (**Fig. 1**). Therefore, SPSB expression in the total absence of SPSA1+SPSA2+SPSC expression is enough to guarantee plant viability.

During the process of generation of the *spsa1/spsa2/spsb/spsc* quadruple mutant we produced the *spsb/spsc* double mutant heterozygous for the *spsa1* and *spsa2* mutations (*spsb/spsc/het-spsa1/het-spsa2*) and the *spsa2/spsb/spsc* triple mutant heterozygous for the *spsa1* mutation (*spsa2/spsb/spsc/het-spsa1*). PCR analyses of 300 plants of the progeny of self-crossed *spsb/spsc/het-spsa1/het-spsa2* and *spsa2/spsb/spsc/het-spsa1* mutants did not allow us to identify any viable *spsa1/spsa2/spsb/spsc* plant. Noteworthy, some of the seeds produced by self-crossed *spsb/spsc/het-spsa1/het-spsa2* and *spsa2/spsb/spsc/het-spsa1* mutants poorly germinated in MS with or without sucrose supplementation, and produced plants with an extremely reduced size and aberrant growth phenotype that were unable to produce flowers (**Fig. 1A**). PCR analyses revealed that these plants were *spsa1/spsa2/spsb/spsc* mutants (**Fig. S3**). These analyses also revealed that some of the aberrant plants obtained from seeds produced by the self-crossed *spsb/spsc/het-spsa1/het-spsa2* mutant possessed a *spsa1/spsb/spsc* genotype (**Fig. S3**). The overall data thus provided strong evidence that (a) SPSA1, SPSB and SPSC play overlapping functions in processes that are essential for normal seed development and germination and subsequent development of the plant, and (b) SPSA2 expression does not compensate the detrimental effects caused by the complete loss of SPSA1+SPSB+SPSC expression.

3.2. Gas exchange analyses of double and triple AtSPS knockout mutants

A_n, Ci and g_s in leaves of viable *sps* mutants (including the *spsa1/spsa2, spsa1/spsb, spsa1/spsc, spsa2/spsb, spsa2/spsc, spsb/spsc*, *spsa1/spsa2/spsc, spsa1/spsa2/spsb* and *spsa2/spsb/spsc* mutants) cultured under ambient CO_2 levels and either 90 µmol photons s^{-1} m^{-2} or saturating light (350 µmol photons s^{-1} m^{-2}) were comparable to those of WT plants (**Fig. S6**). Dark respiration in leaves of all *sps* mutants except *spsa1/spsc* and *spsa1/spsa2/spsc* was normal when compared with that of WT leaves (**Fig. 2**). In clear contrast, dark respiration in leaves of *spsa1/spsc* and *spsa1/spsa2/spsc* was exceedingly higher than that of WT plants (**Fig. 2**) indicating that SPSA1 and SPSC play overlapping functions that are important for plant respiration.

3.3. Metabolic characterization of double and triple AtSPS knockout mutants

We measured the levels of metabolites closely linked to sucrose and starch metabolism (starch, maltose, sucrose, glucose, fructose, G1P, G6P, S6P, UDPG and ADPG) in leaves of all viable *sps* mutants cultured under 16 h light/8 h dark photoperiod conditions. Because of their aberrant growth and extremely reduced size, non-viable *spsa1/spsb/spsc* and *spsa1/spsa2/spsb/spsc* mutants could not be included in this study. As shown in **Fig. 3**, soil-grown *spsa1/spsa2, spsa1/spsb, spsa2/spsb, spsa2/spsc, spsb/spsc, spsa1/spsa2/spsb* and *spsa2/spsb/spsc* mutants accumulated WT levels of nonstructural carbohydrates at the end of the light period, strongly indicating that SPSA1 expression in the total absence of SPSA2+SPSB+SPSC expression, and SPSC expression in the total absence of SPSA1+SPSA2+SPSB expression guarantee normal nonstructural carbohydrate metabolism of the plant.

Sucrose content at the end of the light period in leaves of the *spsa1/spsc* and *spsa1/spsa2/spsc* mutants was ca. 70% of that of WT plants (**Fig. 3**). S6P levels in *spsa1/spsc* and *spsa1/spsa2/spsc* leaves were exceedingly lower than in WT leaves (**Fig. 3**), indicating that SPSA1+SPSC expression is a major determinant of leaf SP6 and sucrose biosynthesis in *Arabidopsis*. Levels of glucose, G1P, G6P and UDPG (all intermediates of the nocturnal starch-to-sucrose conversion pathway, **Fig. S1B**) in *spsa1/spsc* and *spsa1/spsa2/spsc* leaves were 3-4 fold higher than in WT leaves. Noteworthy, maltose content in leaves of *spsa1/spsc* and *spsa1/spsa2/spsc* plants cultured under a 16 h light/8 h dark photoregime were ca. 80- and 100-fold higher than in WT leaves (**Fig. 3**), respectively, which is exceedingly higher than that previously reported using *spsa1/spsc* plants cultured under an 8 h light/16 h dark photoregime [15]. Furthermore, starch content in leaves of *spsa1/spsc* and *spsa1/spsa2/spsc* plants cultured under a 16 h light/8 h dark photoregime was 15-fold higher than in WT leaves, reaching values of 400-450 μmol glucose/g fresh weight (FW) that are comparable to those occurring in reserve organs such as potato tubers [25], and exceedingly higher than those previously reported for *spsa1/spsc* plants cultured under an 8 h light/16 h dark photoregime [15]. Iodine staining analyses were consistent with the presence of high levels of starch in *spsa1/spsc* and *spsa1/spsa2/spsc* leaves (**Fig. S7** and data not shown). Subsequent light microscopy analyses of leaf sections showed that iodine stained starch granules were localized within chloroplasts of mesophyll cells (**Fig. S7** and data not

shown). The overall data strongly indicate that (a) SPSA1, SPSA2 and SPSC overlap in functions that are important for nonstructural carbohydrate metabolism, and (b) there occurs a blockage of the nocturnal starch-to-S6P conversion pathway in *spsa1/spsc* and *spsa1/spsa2/spsc* leaves.

3.4. Enzymatic characterization of multiple AtSPS mutants

We measured the maximum catalytic activities of enzymes closely connected to sucrose and starch metabolism in leaves of all viable *sps* mutants cultured under 16 h light/8 h dark photoperiod conditions. Due to their extremely reduced size and aberrant growth, we could only measure SPS activities in the *spsa1/spsa2/spsb/spsc* mutants. As shown in **Fig. 4,** SPS activities in protein extracts from the *spsa1/spsa2/spsb/spsc* mutant were negligible. Also**,** the maximal extractable SPS activity from mature source leaves of *spsa1/spsc* and *spsa1/spsa2/spsc* plants was ca. 30-35% of the WT activity (**Fig. 4)**. SPS activities in leaves of the *spsa1/spsa2, spsa1/spsb, spsa2/spsb, spsa2/spsc, spsb/spsc, spsa1/spsa2/spsb* and *spsa2/spsb/spsc* mutants were ca. 50-60% of that of WT leaves (**Fig. 4**). Only minor changes likely due to statistical variation were observed for SS, HK, AGP, PPase, SuSy, UGP, acid and alkaline invertases, α-amylase and β-amylase activities in leaves of these mutants (**Fig. S8**). In clear contrast, total PGM activities in leaves of the *spsa1/spsa2, spsa1/spsb, spsa2/spsb, spsa2/spsc, spsb/spsc, spsa1/spsa2/spsb* and *spsa2/spsb/spsc* mutants were 3-5 fold higher than that of WT leaves (**Fig. 4**). Noteworthy, total PGM activity in *spsa1/spsc* and *spsa1/spsa2/spsc* leaves was ca. 20 fold higher than that of WT leaves (**Fig. 4**).

Three PGM isoforms exist in *Arabidopsis*, one in the plastid (PGM1) and two (PGM2 and PGM3) in the cytosol [23,39]. To test which one(s) of the three PGM isoforms(s) is/are up-regulated in the *spsa1/spsc* mutant, we carried out zymogramic analyses of PGM activity on WT and *spsa1/spsc* leaves. As shown in **Fig. S9**, these analyses revealed that the three isoforms were strongly up-regulated in the *spsa1/spsc* mutant when compared with WT plants. Essentially the same results were obtained using the *spsa1/spsa2/spsc* mutant (not shown).

AGP activity is subjected to redox regulation of the small AGP subunit (APS1) [20,40]. Whether changes in redox status of APS1 explain the high starch content

phenotype of *spsa1/spsc* and *spsa1/spsa2/spsc* leaves was investigated by carrying out APS1 immunoblot analyses of proteins from leaves of WT and the *spsa1/spsc* plants that had previously been extracted and electrophoretically separated under non-reducing conditions. In these conditions APS1 is present as a mixture of ca. 50 kDa active (reduced) monomers and ca. 100 kDa inactive (oxidized) dimers formed by intermolecular links involving Cys bridges. Consistent with previous reports [20,40], these analyses revealed that most of APS1 is largely oxidized (inactive) in both WT and *spsa1/spsc* leaves (**Fig. S10**). These analyses also revealed that leaves of the *spsa1/spsc* mutant accumulate identical amounts of ca. 50 kDa monomers and ca. 100 kDa dimers of APS1 than WT leaves, the overall data strongly indicating that the high starch content of *spsa1/spsc* leaves is not ascribed to redox activation of APS1.

3.5. The oxidative pentose phosphate pathway, glycolysis and the tricarboxylic acid cycle are up-regulated in spsa1/spsc leaves

Previous theoretical arguments have proposed that a substantial increase in flux can only be achieved by a co-ordinate up-regulation of a pathway and simultaneous increase of the activity of several enzymes in response to increasing demand for a pathway product [41,42]. The high cytosolic PGM activity (**Fig. 4, Fig. S9**) and the high dark respiration of *spsa1/spsc* and *spsa1/spsa2/spsc* leaves (**Fig. 2)** pointed to the possible activation of the OPPP, glycolysis and/or the respiratory pathways as a possible mechanism to alleviate the blockage of the starch-to-S6P conversion pathway occurring in *spsa1/spsc* and *spsa1/spsa2/spsc* leaves (see above). To test this hypothesis we measured the activities of OPPP enzymes such as PGI, G6PDH, 6PGDH, and glycolytic enzymes such as F1,6P_2 aldolase, G3PDH, 3PGA kinase and PK in leaves of *spsa1/spsc* plants cultured under 16 h light/8 h dark photoperiod conditions. We also analyzed the activities of enzymes of the TCA such as IDH, MDH and SDH. Furthermore, we measured the levels of F6P (a glycolytic and OPPP intermediate), four glycolytic intermediates (F1,6P_2, 3PGA, pyruvate and PEP), and two TCA intermediates (oxalacetate and isocitrate). As shown in **Fig. 5A**, these analyses showed that the levels of glycolytic, OPPP and TCA metabolic intermediates in *spsa1/spsc* leaves were higher than in WT leaves. Not

surprisingly, the activities of enzymes of the glycolytic, OPPP and TCA pathways in *spsa1/spsc* leaves were higher than in WT leaves (**Fig. 5B**).

3.6. spsa1/spsc leaves accumulate high levels of metabolic intermediates of the nocturnal starch-to-sucrose conversion process even under continuous light conditions

Volkert et al. [15] reported that leaves of *spsa1/spsc* plants cultured under 8 h light/16 h dark photoperiod conditions accumulated 3-fold and 6-fold more starch and maltose than WT leaves at the end of the light period, respectively, and concluded that accumulation of maltose (the main starch breakdown product) in *spsa1/spsc* leaves is due to reduced metabolization of maltose into sucrose during the night.

Although it has been proposed that starch breakdown in leaves solely occurs during darkness [43,44], several studies have shown the occurrence of starch breakdown during illumination. Thus, pulse-chase and starch-preloading experiments using isolated chloroplasts [45], intact leaves [16-18,46], or cultured photosynthetic cells [47] have shown that chloroplasts can synthesize and mobilize starch simultaneously (for a review see [48]). Furthermore, recent metabolic flux analyses carried out using illuminated *Arabidopsis* plants cultured in $^{13}CO_2$-enriched environment revealed rapid labeling of maltose [49]. Moreover, enzymes involved in starch breakdown such as GWD, SEX4, isoamylase 3, and plastidic α-amylases 1 and 3 are redox-activated under environmental stress conditions and at physiologically relevant potentials occurring in the illuminated chloroplast [50-53]. Maltose content in leaves of *spsa1/spsc* plants cultured under a 16 h light/8 h dark photoregime (cf. **Fig. 3**) was exceedingly higher than that of leaves of *spsa1/spsc* plants cultured under a 8 h light/16 h dark photoregime [15], pointing to the possible occurrence of very active starch mobilization not only during the night, but also during the light in *spsa1/spsc* leaves. To test this hypothesis we measured the content of maltose-to-sucrose metabolic intermediates in leaves of WT and *spsa1/spsc* plants cultured under continuous light (CL) conditions. We reasoned that, if amylolytic production of maltose and subsequent conversion of this disaccharide into sucrose solely occurs during the dark period, leaves of *spsa1/spsc* plants cultured in the absence of a dark period should accumulate WT levels of maltose. Alternatively, if amylolytic starch breakdown and subsequent conversion of maltose into sucrose also occurs during the day,

levels of maltose and of intermediates in the maltose-to-S6P conversion process in leaves of *spsa1/spsc* plants cultured under CL conditions should be high when compared with WT leaves. Furthermore, due to feedback inhibition of amylolytic breakdown of starch by excess maltose, levels of starch in *spsa1/spsc* leaves should be high when cultured under CL conditions. As shown in **Fig. 6A**, *spsa1/spsc* plants cultured under CL conditions displayed a dwarf phenotype. Furthermore, their leaves accumulated higher levels of G6P, G1P and UDPG than WT leaves, and exceedingly higher levels of starch and maltose than WT leaves (**Fig. 6B**). Expectedly, sucrose and S6P contents in *spsa1/spsc* were lower than in WT leaves (**Fig. 6B**). The overall data thus provided strong evidence that (a) continuously illuminated *spsa1/spsc* leaves degrade starch, and (b) the accumulation of high levels of maltose, G6P, G1P and UDPG, and low levels of sucrose and S6P in leaves of *spsa1/spsc* plants cultured under CL conditions is the consequence of impaired conversion of maltose into S6P.

We also measured maltose and starch contents at the end of the light and dark periods in leaves of WT and *spsa1/spsc* plants cultured under three different photoregimes (12 h light/12 h dark, 16 h light/8 h dark and 20 h light/4 h dark), and compared them with those of leaves of plants cultured under CL conditions. As shown in **Fig. 7,** irrespective of the photoregime, WT and *spsa1/spsc* leaves accumulated lower levels of starch and higher levels of maltose at the end of the dark period than at the end of the light period, indicating the occurrence of amylolytic starch breakdown during the night. Furthermore, irrespective of the photoperiod condition and day moment, starch and maltose contents in *spsa1/spsc* leaves were exceedingly higher than those of WT leaves. Such differences in maltose and starch contents between leaves of WT and *spsa1/spsc* plants cultured under 12 h light/12 h dark, 16 h light/8 h dark and 20 h light/4 h dark photoregimes were much more pronounced than those occurring between leaves of WT and *spsa1/spsc* plants cultured under 8 h light/16 h dark photoperiod conditions ([15] and data not shown). Moreover, maltose and starch contents at the end of the light period in leaves of *spsa1/spsc* plants cultured under 16 h light/8 h dark and 20 h light/4 h dark photoregimes were similar to those of leaves of *spsa1/spsc* plants cultured under CL conditions (**Fig. 7**). The overall data thus strongly indicate that amylolytic production of maltose occurs not only during the night, but also during the day in *spsa1/spsc* leaves.

4. Discussion

Results presented in this work describing the phenotypic and metabolic characteristics of different multiple *SPS* knockout mutants (summarized in **Table S1**) provide strong evidence that (a) the four SPS isoforms overlap in functions that are essential for normal seed development and germination and subsequent development of the plant, (b) the four SPS isoforms play redundant functions in process that are important for nonstructural carbohydrate metabolism (c) SPSA2 expression does not compensate the detrimental effects caused by the complete loss of SPSA1+SPSB+SPSC expression, (d) SPSB expression in the total absence of SPSA1+SPSA2+SPSC expression is enough to guarantee plant viability, and (e) SPSA1 expression in the total absence of SPSA2+SPSB+SPSC expression, and SPSC expression in the total absence of SPSA1+SPSA2+SPSB expression guarantee normal development, growth and nonstructural carbohydrate metabolism of the plant. That (a) the *spsa1/spsc* mutant has a reduced vegetative and reproductive growth phenotype that is exacerbated in the *spsa1/spsa2/spsc* mutant, and (b) the *spsa1/spsb/spsc* and *spsa1/spsa2/spsb/spsc* mutants (both totally lacking *SPSA1* and *SPSC* expression) are not viable (**Fig. 1**) strongly indicates that SPSA1 and SPSC (and to a lesser extent SPSA2 and SPSB) play predominant roles in processes that are important for fertility, development and growth. This is further strengthen by the observations that the *spsa1/spsa2/spsb* and *spsa2/spsb/spsc* mutants display a WT phenotype and produce fertile seeds (**Fig. 1** and data not shown).

In vitro, SuSy catalizes the reversible conversion of sucrose and NDP into the corresponding NDPG and fructose [48]. It primarily works as a sucrose-degrading enzyme *in planta,* playing important roles in the regulation of carbon partitioning into various sink tissues or organs and in phloem loading and unloading. Although SuSy can potentially synthesize sucrose from UDPG and fructose, results presented in this work showing that (a) *spsa1/spsa2/spsb/spsc* mutants are not viable **(Fig. 1)**, and (b) *spsa1/spsc* and *spsa1/spsa2/spsc* leaves accumulate reduced levels of sucrose (**Fig. 3**), provide strong evidence that (a) SuSy plays a minor role, if any, in the sucrose biosynthetic process, and (b) sucrose is mainly synthesized through the SPS-SPP pathway in *Arabidopsis*.

Comparative studies of *SPS* gene expression in *Arabidopsis* using quantitative RT-PCR and promoter-reporter gene expression techniques showed that *SPSA1* is expressed in all tissues except roots and, together with *SPSC,* constitutes the major *SPS* gene expressed in leaves [14,15]. *SPSA2* is mainly expressed in roots, whereas *SPSB* is predominantly expressed in seeds and reproductive organs [14,15]. In addition, genome-wide expression analyses (https://www.geneinvestigator.ethz.ch, [54]) showed strong expression of *SPSA1* in most organs and tissues, medium/moderate expression levels of *SPSA2, SPSB* and *SPSC* in most organs and tissues, and high expression of *SPSB* in seeds. It is thus conceivable that the poor germination and aberrant growth of *spsa1/spsb/spsc* is due to impairments in processes mediated by SPSA1, SPSB and SPSC that are essential for fertilization and/or seed development and subsequent development and growth of the plant.

Recently, Brauner et al. [55] reported that growth reduction in near-starchless *pgm1* mutants impaired in pPGM is caused by exaggerated root respiration. Taking into account that respiration in *spsa1/spsc* and *spsa1/spsa2/spsc* plants is exceedingly higher than in WT plants (**Fig. 2**) it is highly conceivable that restricted growth of these mutants (**Figs. 1** and **6**) is ascribed not only to impairments in leaf sucrose synthesis and subsequent provision of photosynthate to the rest of the plant, but also to exaggerated respiration. The stunted growth phenotype and high maltose content of the *spsa1/spsc* and *spsa1/spsa2/spsc* mutants (**Fig. 1**) is reminiscent of that observed in the *mex1* and *dpe2* mutants whose phenotypes have been ascribed to impairment in the maltose to sucrose conversion process during the night [6-8]. Results presented in this work showing that (a) the levels of all metabolic intermediates in the nocturnal maltose to S6P conversion pathway in *spsa1/spsc* leaves are higher than in WT leaves when plants are cultured under CL conditions (**Fig. 6**), (b) maltose contents at the end of the light period in leaves of *spsa1/spsc* plants cultured under different photoregimes are similar to those of leaves of *spsa1/spsc* plants cultured under CL conditions (**Fig. 7B),** and (c) the levels of glycolytic, OPPP and TCA metabolic intermediates and enzymatic activities in *spsa1/spsc* leaves are higher than in WT leaves (**Fig. 5**) point to the occurrence in *spsa1/spsc* leaves of mechanism(s) involving simultaneous synthesis and mobilization of starch during the day similar to that previously reported for mutants impaired in TPT [16-

18], and channeling of starch breakdown products towards the glycolytic, OPPP and TCA as schematically illustrated in **Fig. S11**. Previous studies have shown that enhancement of plastidic PGM stimulates photosynthetic carbon flow into starch [56]. It is thus conceivable that elevated plastidic PGM occurring in *spsa1/spsc* and *spsa1/spsa2/spsc* plants (**Fig. 4** and **Fig. S9**) will favor the scavenging of starch breakdown products, thus making up a substrate (starch) cycle. Both activation of starch cycling and enhanced respiration can be considered as alleviation mechanisms that would contribute to compensate the detrimental effects caused by the blockage of sucrose biosynthesis in *spsa1/spsc* and *spsa1/spsa2/spsc* leaves.

ACKNOWLEDGEMENTS

This work was partially supported by the Comisión Interministerial de Ciencia y Tecnología and Fondo Europeo de Desarrollo Regional (Spain) [grant numbers BIO2010-18239, BIO2013-49125-C2-1-P, BIO2008-02292 and BIO2011-28847-C02-02]. A.M.S-L. acknowledges a predoctoral fellowship from the Spanish Ministry of Science and Innovation. M.B. acknowledges a post-doctoral fellowship from the Public University of Navarra.

REFERENCES

1. I. Ciereszko, H. Johansson, L.A. Kleczkowski, Sucrose and light regulation of a cold-inducible UDP-glucose pyrophosphorylase gene via a hexokinase-independent and abscisic acid-insensitive pathway in Arabidopsis, Biochem. J. 354 (2001) 67-82.
2. M. Zourelidou, M. de Torres-Zabala, C. Smith, M.W. Bevan, Storekeeper defines a new class of plant-specific DNA-binding proteins and is a putative regulator of patatin expression, Plant J. 30 (2002) 489-497.
3. M.A. Blázquez, R. Green, O. Nilsson, M.R. Sussman, D. Weigel, Gibberelins promote flowering of Arabidopsis by activating the LEAFY promoter, Plant Cell 10 (1998) 791-800.
4. R.W. King, Y. Ben-Tal, A florigenic effect of sucrose in *Fuchsia hydrida* is blocked by gibberellin-induced assimilate competition, Plant Physiol. 125 (2001) 488-496.
5. D. Iraqi, F.M. Tremblay, Analysis of carbohydrate metabolism enzymes and cellular contents of sugars and proteins during spruce somatic embryogenesis suggests a regulatory role of exogenous sucrose in embryo development, J. Exp. Bot. 52 (2001) 2301-2311.
6. T. Chia, D. Thorneycroft, A. Chapple, G. Messerli, J. Chen, et al., A cytosolic glucosyltransferase is required for conversion of starch to sucrose in *Arabidopsis* leaves at night, Plant J. 37 (2004) 853-863.
7. T. Niittylä, G. Messerli, M. Trevisan, J. Chen, C. Smith, et al., A previously unknown maltose transporter essential for starch degradation in leaves, Science 303 (2004) 87-89.
8. S.E. Weise, K.S. Kim, R.P. Stewart, T.D. Sharkey, β-maltose is the metabolically active anomer of maltose during transitory starch degradation, Plant Physiol. 137 (2005) 756-761.
9. M.H. Cho, H. Lim, D.H. Shin, J.S. Jeonv, S.H. Bhoo, et al., Role of the plastidic glucose translocator in the export of starch degradation products from the chloroplasts in *Arabidopsis thaliana*, New Phytol. 109 (2011) 101-112.

10. S.C. Huber, J.L. Huber, Role and regulation of sucrose-phosphate synthase in higher plants, Ann. Rev. Plant Physiol. Plant Mol. Biol. 47 (1996) 431-444.
11. H. Winter, S.C. Huber, Regulation of sucrose metabolism in higher plants: localization and regulation of activity of key enzymes, Crit. Rev. Plant Sci. 19 (2000) 31-67.
12. Y. Gibon, O.E. Bläsing, N. Palacios-Rojas, D. Pankovic, J.H.M. Hendriks, et al., Adjustment of diurnal starch turnover to short days: inhibition of carbohydrate utilization, accumulation of sugars and post-translational activation of ADP-glucose pyrophosphorylase in the following light period, Plant J. 39 (2004) 847-862.
13. M. Okamura, N. Aoki, T. Hirose, M. Yonekura, C. Ohto, et al., Tissue specific and diurnal change in gene expression of the sucrose phosphate synthase gene family in rice, Plant Sci. 181 (2011) 159-166.
14. J. Sun, J. Zhang, C. Larue, S. Huber, Decrease in leaf sucrose synthesis leads to increased leaf starch turnover and decreased RuBP regeneration-limited photosynthesis but not Rubisco-limited photosynthesis in *Arabidopsis* null mutants of *SPSA1*, Plant Cell Environ. 34 (2011) 592-604.
15. K. Volkert, S. Debast, L.M. Voll, H. Voll, I. Schießl, et al., Loss of the two major leaf isoforms of sucrose-phosphate synthase in *Arabidopsis thaliana* limits sucrose synthesis and nocturnal starch degradation but does not alter carbon partitioning during photosynthesis, J. Exp. Bot. 65 (2014) 5217-5229.
16. R.E. Häusler, N.H. Schlieben, B. Schulz, U.-I. Flügge, Compensation of decreased triose phosphate/phosphate translocator activity by accelerated starch turnover and glucose transport in transgenic tobacco, Planta 204 (1998) 366-376.
17. A. Schneider, R.E. Häusler, Ü. Kolukisaoglu, R. Kunze, E. van der Graaff, et al., An *Arabidopsis thaliana* knock-out mutant of the chloroplast triose phosphate/phosphate translocator is severely compromised only when starch synthesis, but not starch mobilization is abolished, Plant J. 32 (2002) 685-699.
18. R.G. Walters, D.G. Ibrahim, P. Horton, N.J. Kruger, A mutant of *Arabidopsis* lacking the triose-phosphate/phosphate translocator reveals metabolic regulation of starch breakdown in the light, Plant Physiol. 135 (2004) 891-906.

19. J.A. Rojas-González, M. Soto-Suárez, A. García-Díaz, M.C. Romero-Puertas, L.M. Sandalio, et al., Disruption of both chloroplastic and cytosolic FBPase genes results in a dwarf phenotype and important starch and metabolite changes in *Arabidopsis thaliana*, J. Exp. Bot. 66 (2015) 2673-2689.
20. J. Li, G. Almagro, F.J. Muñoz, E. Baroja-Fernández, A. Bahaji, et al., Posttranslational redox modification of ADP-glucose pyrophosphorylase in response to light is not a major determinant of fine regulation of leaf starch accumulation in Arabidopsis, Plant Cell Physiol. 53 (2012) 433-444.
21. T.W.A. Jones, L.D. Gottlieb, E. Pichersky, Reduced enzyme activity and starch level in an induced mutant of chloroplast phosphoglucose isomerase, Plant Physiol. 81 (1986) 367-371.
22. E. Baroja-Fernández, F.J. Muñoz, J. Li, A. Bahaji, G. Almagro, et al., Sucrose synthase activity in the *sus1/sus2/sus3/sus4* Arabidopsis mutant is sufficient to support normal cellulose and starch production, Proc. Natl. Acad. Sci. U.S.A. 109 (2012) 321-326.
23. T. Caspar, S.C. Huber, C. Somerville, Alterations in growth, photosynthesis, and respiration in a starchless mutant of *Arabidopsis thaliana* (L.) deficient in chloroplast phosphoglucomutase activity, Plant Physiol. 79 (1985) 11-17.
24. X. Liu, S. Zhang, X. Shan, Y.G. Zhu, Toxicity of arsenate and arsenite on germination, seedling growth and amylolitic activity of wheat, Chemosphere 61 (2005) 293-301.
25. E. Baroja-Fernández, F.J. Muñoz, M. Montero, E. Etxeberria, M.T. Sesma, et al., Enhancing sucrose synthase activity in transgenic potato (*Solanum tuberosum* L.) tubers results in increased levels of starch, ADPglucose and UDPglucose and total yield, Plant Cell Physiol. 50 (2009) 1651-1662.
26. A. Renz, L. Merlo, M. Stitt, Partial purification from potato tubers of three fructokinases and three hexokinases which show differing organ and developmental specificity, Planta 190 (1993) 156-165.
27. E. Baroja-Fernández, F.J. Muñoz, A. Zandueta-Criado, M.T. Morán-Zorzano, A.M. Viale, et al., Most of ADP-glucose linked to starch biosynthesis occurs outside the

chloroplast in source leaves, Proc. Natl. Acad. Sci. U.S.A. 101 (2004) 13080-13085.

28. J. Li, E. Baroja-Fernández, A. Bahaji, F.J. Muñoz, M. Ovecka, et al., Enhancing sucrose synthase activity results in increased levels of starch and ADP-glucose in maize (*Zea mays* L.) seed endosperms, Plant Cell Physiol. 54 (2013) 282-294.
29. M.M. Burrell, P.J. Mooney, M. Blundy, D. Carter, F. Wilson, et al., Genetic manipulation of 6-phosphofructokinase in potato tubers, Planta 194 (1994) 95-101.
30. M. Leterrier, J.B. Barroso, R. Valderrama, J.M. Palma, F.J. Corpas, NADP-dependent isocitrate dehydrogenase from Arabidopsis roots contributes in the mechanism of defence against the nitro-oxidative stress induced by salinity, ScientificWorldJournal (2012) 694740. doi: 10.1100/2012/694740.
31. T. Tomaz, M. Bargard, I. Pracharoenwattana, P. Lindén, C.P. Lee, et al., Mitochondrial malate dehydrogenase lowers leaf respiration and alters photorespiration in plant growth in *Arabidopsis*, Plant Physiol. 154 (2010) 1143-1157.
32. S. Huang, N.L. Taylor, E. Ströher, R. Fenske, A.H. Millar, Succinate dehydrogenase assembly factor 2 is need for assembly and activity of mitochondrial complex II and for normal root elongation in *Arabidopsis*, Plant J. 73 (2013) 429-441.
33. A. Bahaji, E. Baroja-Fernández, A.M. Sánchez-López, F.J. Muñoz, J. Li, et al., HPLC-MS/MS analyses show that the near-starchless *aps1* and *pgm* leaves accumulate wild type levels of ADPglucose: further evidence for the occurrence of important ADPglucose biosynthetic pathway(s) alternative to the pPGI-pPGM-AGP pathway, PLOS ONE 18;9(8) (2014) e104997.
34. A. Lytovchenko, K Bieberich, L. Willmitzer, A.R. Fernie, Carbon assimilation and metabolism in potato leaves deficient in plastidial phosphoglucomutase, Planta 215 (2002) 802-811.
35. L.J. Sweetlove, M.M. Burrell, T. ap Rees, Starch metabolism in tubers of transgenic potato (*Solanum tuberosum*) with increased ADPglucose pyrophosphorylase, Biochem. J. 320 (1996) 493-498.

36. L.-S. Chen, Q. Lin, A. Nose, A comparative study on diurnal changes in metabolite levels in the leaves of three ceassulacean acid metabolism (CAM) species, *Ananas comosus, Kalanchoë daigremontiana* and *K. pinnata*, J. Exp. Bot. 53 (2002) 341-350.
37. S. von Caemmerer, G.D. Farquhar, Some relationships between the biochemistry and photosynthesis and the gas exchange of leaves, Planta 153 (1981) 376-387.
38. P.C. Harley, F. Loreto, G.D. Marco, T.D. Sharkey, Theoretical considerations when estimating the mesophyll conductance to CO_2 flux by analysis of the response of photosynthesis to CO_2, Plant Physiol. 98 (1992) 1429-1436.
39. B. Egli, K. Kölling, C. Köhler, S.C. Zeeman, S. Streb, Loss of cytosolic phosphoglucomutase compromises gametophyte development in Arabidopsis, Plant Physiol. 154 (2010) 1659-1671.
40. J.H.M. Hendriks, A. Kolbe, Y. Gibon, M. Stitt, P. Geigenberger, ADP-glucose pyrophosphorylase is activated by posttranslational redox-modification in response to light and to sugars in leaves of *Arabidopsis* and other plant species, Plant Physiol. 133 (2003) 838-849.
41. A. Cornish-Bowden, J.H.S. Hofmeyr, M.L. Cárdenas, Strategies for manipulating metabolic fluxes in biotechnology, Bioorg. Chem. 23 (1995) 439-449.
42. S. Thomas, P.J.F. Mooney, M.M. Burrell, D.A. Fell, Finite changes analysis of glycolytic intermediates in tuber tissue of lines of transgenic potato (*Solanum tuberosum*) overexpressing phosphofructokinase, Biochem. J. 322 (1997) 111-117.
43. S.C. Zeeman, A. Tiessen, E. Pilling, K.L. Kato, A.M. Donald, et al., Starch synthesis in Arabidopsis. Granule synthesis, composition, and structure, Plant Physiol. 129 (2002) 516-529.
44. M. Stitt, S.C. Zeeman, Starch turnover: pathways, regulation and role in growth, Curr. Opin. Plant Biol. 15 (2012) 1-11.
45. M. Stitt, H.W. Heldt, Simultaneous synthesis and degradation of starch in spinach chloroplasts in the light, Biochim. Biophys. Acta 638 (1981) 1-11.
46. T.C. Fox, D.R. Geiger, Effects of decreased net carbon exchange on carbohydrate metabolism in sugar beet source leaves, Plant Physiol. 76 (1984) 763-768.

47. V.V. Lozovaya, O.A. Zabotina, J.M. Widholm, Synthesis and turnover of cell-wall polysaccharides and starch in photosynthetic soybean suspension cultures, Plant Physiol. 111 (1996) 921-929.
48. A. Bahaji, J. Li, A.M. Sánchez-López, E. Baroja-Fernández, F.J. Muñoz, et al., Starch biosynthesis, its regulation and biotechnological approaches to improve crop yields. Biotechnol. Adv. 32 (2014) 87-106.
49. M. Szecowka, R. Heise, T. Tohge, A. Nunes-Nesi, D. Vosloh, et al., Metabolic fluxes in an illuminated *Arabidopsis* rosette, Plant Cell 25 (2013) 694-714.
50. R. Mikkelsen, K.E. Mutenda, A. Mant, P. Schürmann, A. Blennow, α-glucan, water dikinase (GWD): a plastidic enzyme with redox-regulated and coordinated catalytic activity and binding affinity, Proc. Natl. Acad. Sci. U.S.A. 102 (2005) 1785-1790.
51. F. Sparla, A. Costa, F. Lo Schiavo, P. Pupillo, P. Trost, Redox regulation of a novel plastid-targeted β-amylase of Arabidopsis, Plant Physiol. 141 (2006) 840-850.
52. C. Valerio, A. Costa, L. Marri, E. Issakidis-Bourguet, P. Pupillo, et al., Thioredoxin-regulated β-amylase (BAM1) triggers diurnal starch degradation in guard cells, and in mesophyll cells under osmotic stress, J. Exp. Bot. 62 (2010) 545-555.
53. M.A. Glaring, K. Skryhan, O. Kötting, S.C. Zeeman, A. Blennow, Comprehensive survey of redox sensitive starch metabolizing enzymes in *Arabidopsis thaliana*, Plant Physiol. Biochem. 58 (2012) 89-97.
54. P. Zimmermann, M. Hirsch-Hoffmann, L. Hennig, W. Gruissem, GENEVESTIGATOR. Arabidopsis microarray database and analysis toolbox, Plant Physiol. 136 (2004) 2621-2632.
55. K. Brauner, I. Hörmiller, T. Nägele, A.G. Heyer, Exaggerated root respiration accounts for growth retardation in a starchless mutant of *Arabidopsis thaliana*, Plant J. 79 (2014) 82-91.
56. K. Uematsu, N. Suzuki, T. Iwamae, M. Inui, H. Yukawa, Expression of Arabidopsis plastidial phosphoglucomutase in tobacco stimulates photosynthetic carbon flow into starch synthesis, J. Plant Physiol. 169 (2012) 1454-1462.

FIGURE LEGENDS

Fig. 1: Morphology and growth phenotype of *sps* mutants. (A) Morphology of WT plants and the indicated *sps* mutants at 24 days after germination (DAG). (B) Time-course of rosette FW of WT plants and the indicated *sps* mutants. (C) Morphology of flowers and siliques of WT and the indicated *sps* mutants**.** Values represent the mean of determinations on five different rosettes. Plants were cultured on soil under 16 h light/8 h dark conditions.

Fig. 2: Respiratory CO_2 production in darkened source leaves of WT and different viable *sps* plants. Plants were cultured on soil under 16 h light/8 h dark conditions. Values represent the mean ± SE of determinations on four independent samples.

Fig. 3: Metabolites content in leaves of WT plants and different viable *sps* mutants. Fully developed leaves of 30 DAG plants cultured on soil under 16 h light/8 h dark conditions were harvested after 16 h of illumination. Values represent the mean ± SE of determinations on five independent samples. Each sample included leaves from 3 different rosettes. Asterisks indicate significant differences based on Student´s t-tests. ($P<0.05$, *sps* mutants vs. WT).

Fig. 4: SPS and PGM activities in leaves of WT and different viable *sps* mutants. Fully developed leaves of 30 DAG plants cultured on soil under 16 h light/8 h dark conditions were harvested after 16 h of illumination. Values represent the mean ± SE of determinations on five independent samples. Each sample included leaves from 3 different rosettes. Asterisks indicate significant differences based on Student´s t-tests. ($P<0.05$, *sps* mutants vs. WT).

Fig. 5: Metabolic characterization of WT and *spsa1/spsc* leaves. (A) Levels of glycolytic, OPPP and TCA metabolic intermediates. (B) Activities of enzymes of the glycolytic, OPPP and TCA pathways. Fully developed leaves of 30 DAG plants cultured on soil under 16 h light/8 h dark conditions were harvested after 16 h of illumination. Levels of TCA intermediates were measured using leaves harvested at the end of the dark

period. Values represent the mean ± SE of determinations on five independent samples. Each sample included leaves from 3 different rosettes.

Fig. 6: Characterization of WT and *spsa1/spsc* plants cultured on soil under CL conditions. (A) Morphology of WT and *spsa1/spsc* plants. (B) Metabolic characterization of leaves of 30 DAG WT and *spsa1/spsc* plants. In "B", values represent the mean ± SE of determinations on five independent samples. Each sample included leaves from 3 different rosettes.

Fig. 7: *spsa1/spsc* leaves accumulate high levels of maltose and starch even under continuous light conditions. (A) Starch and (B) maltose contents at the end of the light and dark periods in leaves of WT and *spsa1/spsc* plants cultured under three different photoregimes (12 h light/12 h dark, 16 h light/8 h dark and 20 h light/4 h dark), and under CL conditions. Dark bars represent values of starch and maltose contents in leaves harvested at the end of the dark period. White bars represent values of starch and maltose contents in leaves harvested at the end of the light period. Values represent the mean ± SE of determinations on five independent samples. Each sample included leaves from 3 different rosettes. Inset in "B" shows maltose content in WT leaves at the end of the dark and light periods.

SUPPLEMENTAL INFORMATION LEGENDS

Table S1: *sps* mutants used in this work and their phenotypes.

Table S2: Primers used for PCR screening of *sps* mutants.

Table S3: Primers used in RT-PCR analyses

Fig. S1: Metabolic schemes of sucrose biosynthesis in leaves (A) during the day, and (B) during the night. During the day, photosynthetically fixed carbon is either retained within the chloroplast to fuel the synthesis of transitory starch, or exported to the cytosol as triose phosphates by means of TPT to be subsequently converted into sucrose. During the night, starch is remobilized thereby providing maltose and glucose molecules that are metabolized to support sucrose synthesis and growth. The enzyme activities involved are numbered as follows: 1, 1′, fructose-1,6-bisphosphate aldolase; 2, 2′, fructose 1,6-bisphosphatase; 3, PPi:fructose-6-phosphate phosphotransferase; 4, 4′, PGI; 5, 5′, PGM; 6, UGP; 7, SPS; 8, SPP; 9, AGP; 10, SS; 11, β-amylase; 12, 12′, DPE; 13, glucan phosphorylase (PHS2); 14, HK. In "B", starch to glucose conversion would involve the coordinated actions of amylases, isoamylase and plastidic DPE (DPE1). Maltose is transported from plastid to the cytosol via the maltose transporter MEX1. Glucose is transported from plastid to the cytosol via the pGlcT glucose translocator.

Fig. S2: Schemes illustrating the structure of *AtSPSA1, AtSPSA2, AtSPSB* and *AtSPSC* and the T-DNA insertion sites in the *spsa1* (SALK_119162), *spsa2* (SALK_064922), *spsb* (GABI_368F01) and *spsc* (SAIL_31_H05) alleles. The schemes also illustrate the positions of LP and RP *SPSA1, SPSA2, SPSB* and *SPSC* specific primers, and the T-DNA specific primers used for PCR confirmation of mutations (see **Table S2**).

Fig. S3: PCR analyses of *sps* mutants. *SPS* LP and RP specific primers, and T-DNA specific primers used are listed in **Table S2.** Annealing positions of *SPS* LP and RP specific primers, and T-DNA specific primers are shown in **Fig S2.**

Fig. S4: RT-PCR analysis for the transcripts of SPS null mutants. 18S RNA was used as the positive control.

Fig. S5: Time-course of FW of rosettes of WT and *spsa1/spsc* plants cultured in solid MS medium with and without 90 mM sucrose supplementation. Plants were cultured under 16 h light/8 h dark conditions. Values represent the mean ± SE of determinations on four independent samples.

Fig. S6: Gas exchange analyses of WT and different viable *sps* mutants. The graphics represent the net CO_2 uptake (A_n), the intercellular CO_2 concentration (Ci) and the stomatal conductance (g_s) in source leaves of WT and *sps* plants cultured on soil under 16 h light/8 h dark conditions under photosynthetic photon flux densities of 90 and 350 µmol m^{-2} s^{-1}. Values represent the mean ± SE of determinations on four independent samples.

Fig. S7: Iodine staining of WT and *spsa1/spsc* plants. Upper panel: Iodine staining of whole plants. Lower panel: Iodine staining of cross sections of leaves. Plants were cultured on soil under 16 h light/8 h dark conditions and harvested 25 DAG.

Fig. S8: Activities of enzymes closely connected to starch and sucrose metabolism in mature leaves of WT plants and *sps* mutants. Plants were cultured on soil under 16 h light/8 h dark conditions. Fully developed source leaves were harvested from 30 DAG plants after 16 h of illumination. Values represent the mean ± SE of determinations on five independent samples. Each sample included leaves from 3 different rosettes.

Fig. S9: PGM zymogram of proteins extracted from WT and *spsa1/spsc* leaves. One hundred µg of proteins were loaded onto each lane.

Fig. S10: Non-reducing western blot of APS1 in leaves of WT and *spsa1/spsc* plants. Plants were cultured under 16 h light/8 h dark conditions and leaves harvested from 30 DAG plants after 16 h of illumination.

Fig. S11: Schematic model illustrating the metabolic diversion in *spsa1/spsc* leaves between starch, sucrose, OPPP, glycolysis and TCA metabolic pathways (A) during the day and (B) during the night. Numbering of enzyme activities 1-14 are the same as in Fig. S1. 15, phosphofructokinase; 16, fructose-1,6-bisphosphate aldolase. Enzymatic activities and pathways that are up-regulated in *spsa1/spsc* leaves are indicated with large arrows.

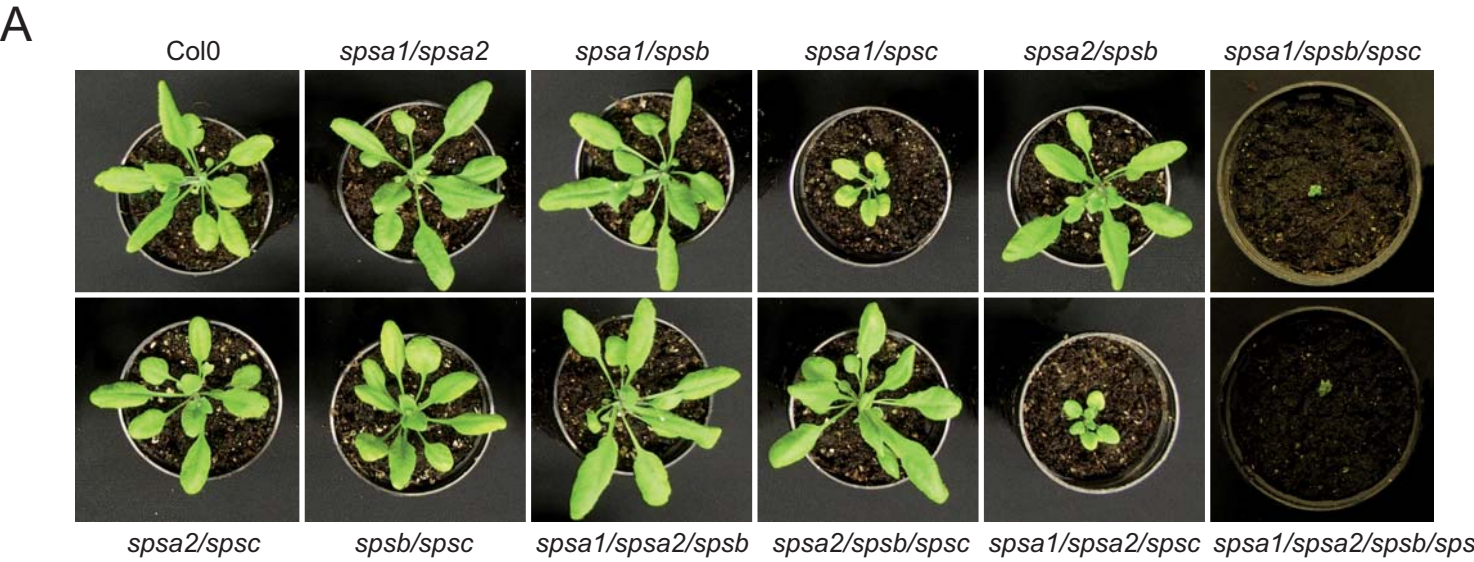
A
Col0
spsa1/spsa2
spsa1/spsb
spsa1/spsc
spsa2/spsb
spsa1/spsb/spsc
spsa2/spsc
spsb/spsc
spsa1/spsa2/spsb
spsa2/spsb/spsc
spsa1/spsa2/spsc
spsa1/spsa2/spsb/spsc

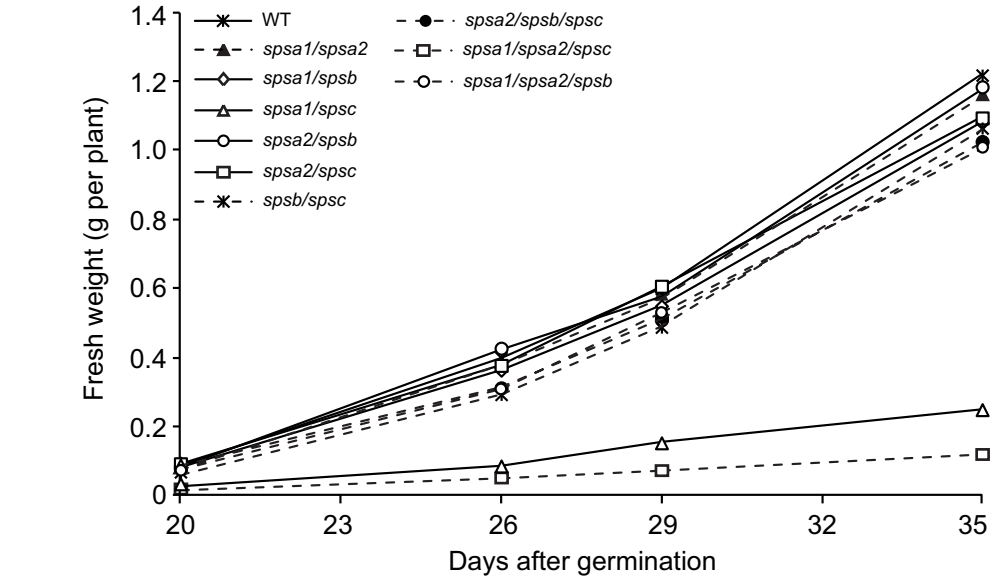
B
WT
spsa1/spsa2
spsa1/spsb
spsa1/spsc
spsa2/spsb
spsa2/spsc
spsb/spsc
spsa2/spsb/spsc
spsa1/spsa2/spsc
spsa1/spsa2/spsb
Fresh weight (g per plant)
1.4
1.2
1.0
0.8
0.6
0.4
0.2
0
20
23
26
29
32
35
Days after germination


C
Col0
spsa1/spsa2/spsb
spsa2/spsb/spsc
spsa1/spsc
spsa1/spsa2/spsc

Figure 1

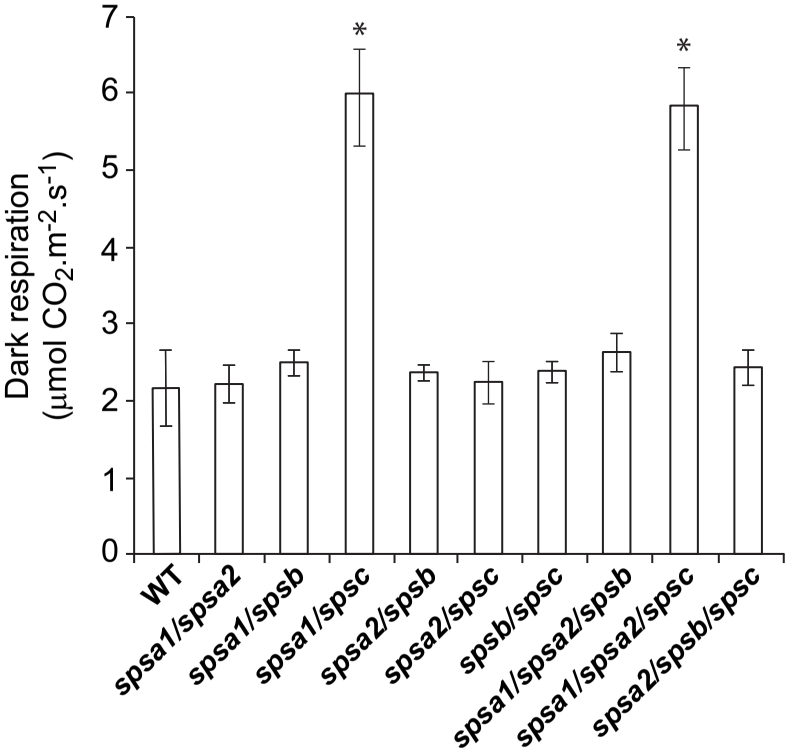
Dark respiration
(µmol CO2.m-2.s-1)
0
1
2
3
4
5
6
7
*
*
WT
spsa1/spsa2
spsa1/spsb
spsa1/spsc
spsa2/spsb
spsa2/spsc
spsb/spsc
spsa1/spsa2/spsb
spsa1/spsa2/spsc
spsa2/spsb/spsc

Figure 2

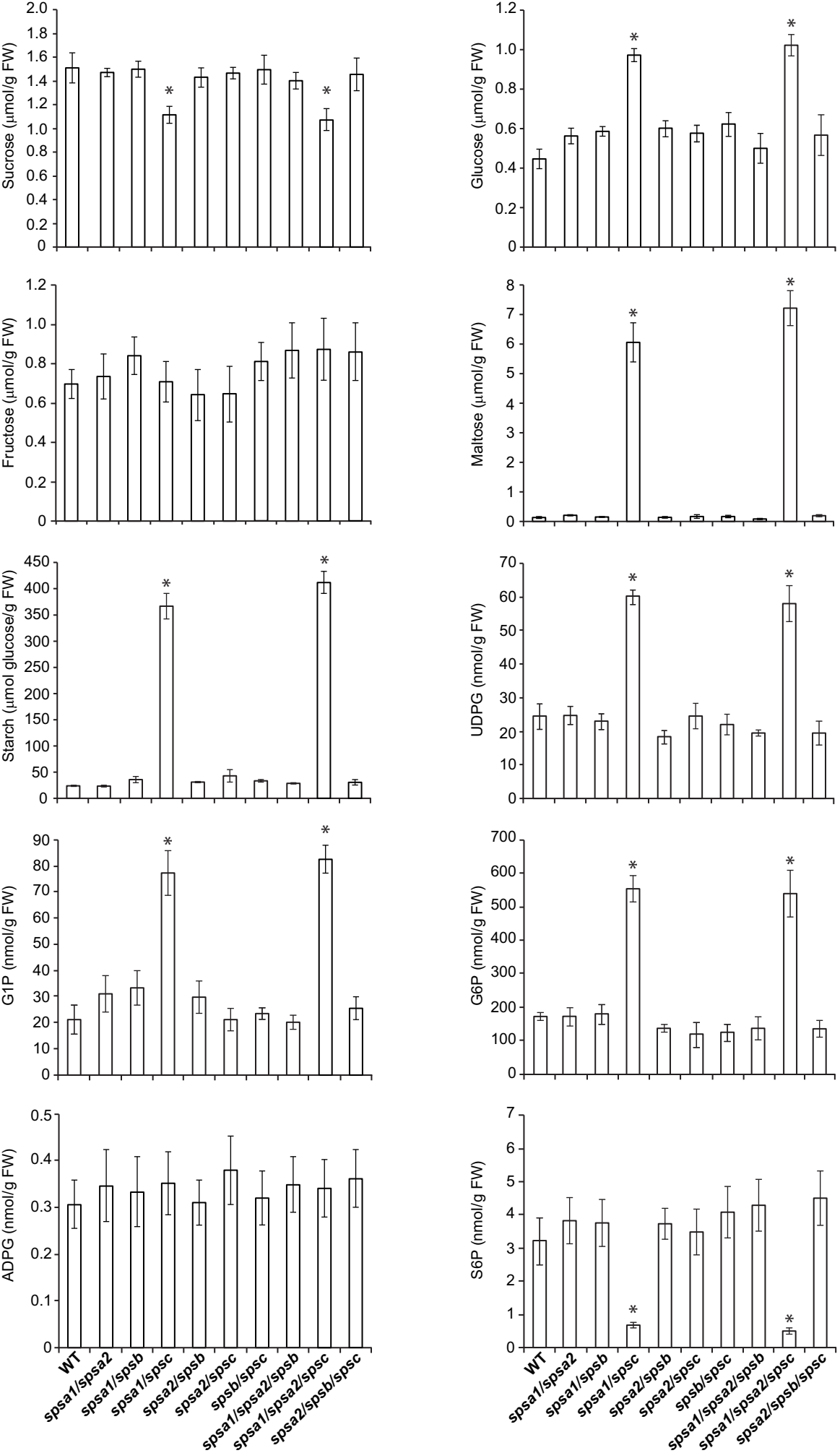
Sucrose (μmol/g FW)
Glucose (μmol/g FW)
Fructose (μmol/g FW)
Maltose (μmol/g FW)
Starch (μmol glucose/g FW)
UDPG (nmol/g FW)
G1P (nmol/g FW)
G6P (nmol/g FW)
ADPG (nmol/g FW)
S6P (nmol/g FW)
WT
spsa1/spsa2
spsa1/spsb
spsa1/spsc
spsa2/spsb
spsa2/spsc
spsb/spsc
spsa1/spsa2/spsb
spsa1/spsa2/spsc
spsa2/spsb/spsc

Figure 3

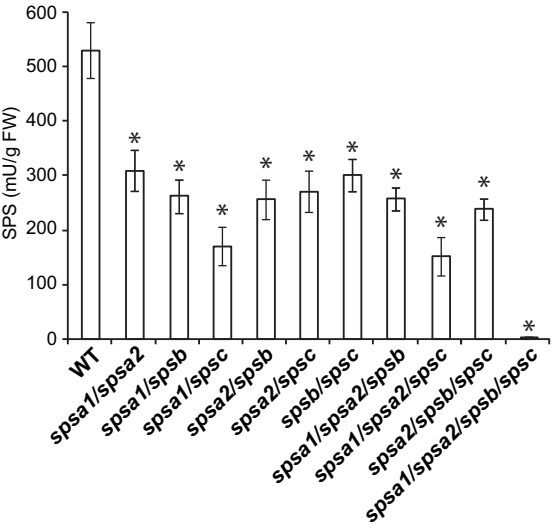
SPS (mU/g FW)
600
500
400
300
200
100
0
*
WT
spsa1/spsa2
spsa1/spsb
spsa1/spsc
spsa2/spsb
spsa2/spsc
spsb/spsc
spsa1/spsa2/spsb
spsa1/spsa2/spsc
spsa2/spsb/spsc
spsa1/spsa2/spsb/spsc

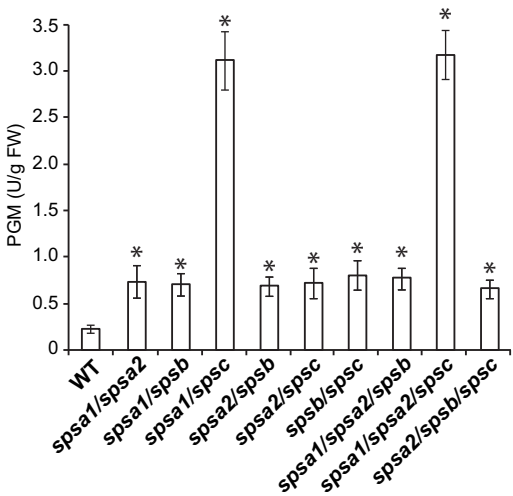
PGM (U/g FW)
3.5
3.0
2.5
2.0
1.5
1.0
0.5
0
*
WT
spsa1/spsa2
spsa1/spsb
spsa1/spsc
spsa2/spsb
spsa2/spsc
spsb/spsc
spsa1/spsa2/spsb
spsa1/spsa2/spsc
spsa2/spsb/spsc

Figure 4

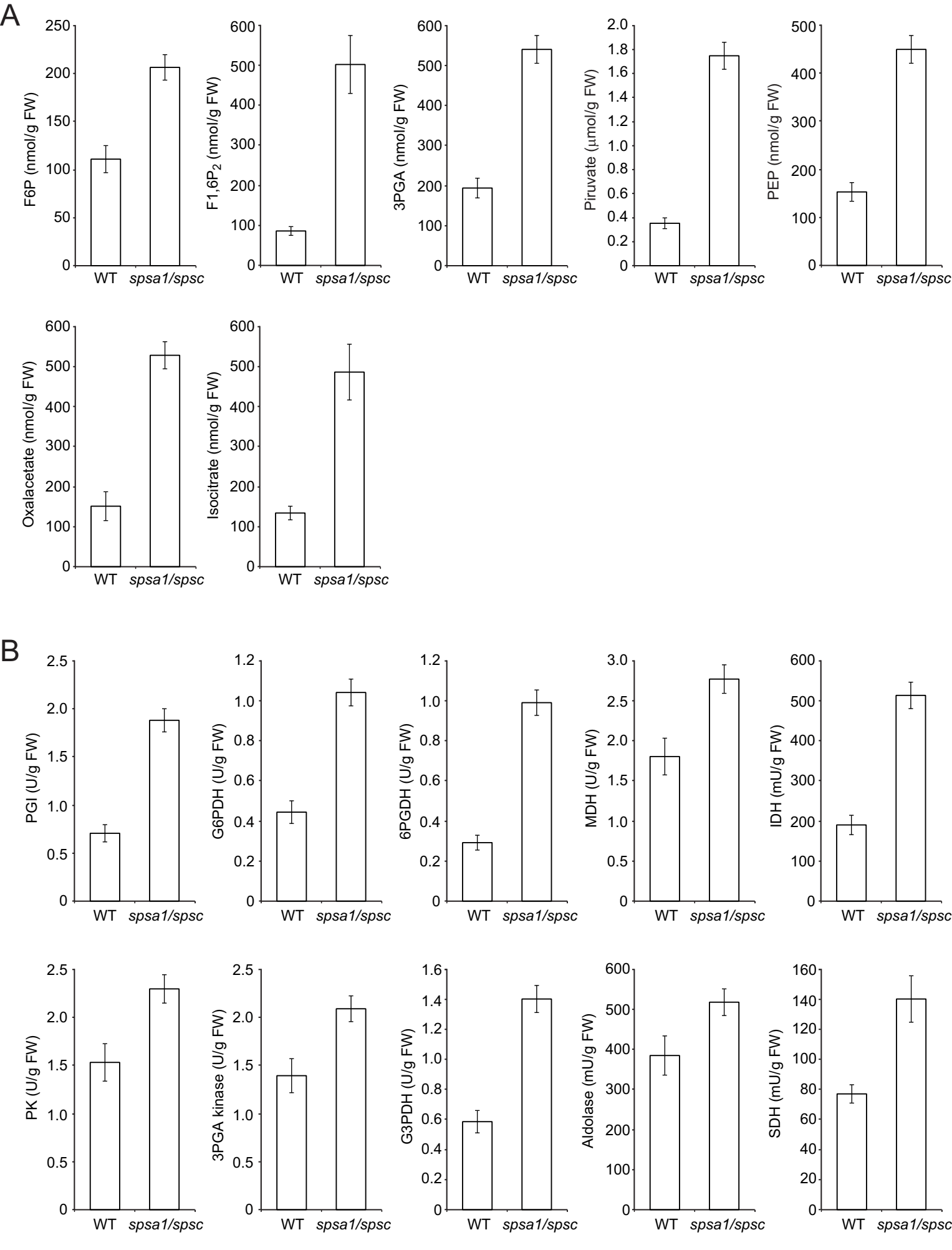
A
F6P (nmol/g FW)
F1,6P2 (nmol/g FW)
3PGA (nmol/g FW)
Piruvate (µmol/g FW)
PEP (nmol/g FW)
Oxalacetate (nmol/g FW)
Isocitrate (nmol/g FW)
WT
spsa1/spsc
B
PGI (U/g FW)
G6PDH (U/g FW)
6PGDH (U/g FW)
MDH (U/g FW)
IDH (mU/g FW)
PK (U/g FW)
3PGA kinase (U/g FW)
G3PDH (U/g FW)
Aldolase (mU/g FW)
SDH (mU/g FW)

Figure 5

A

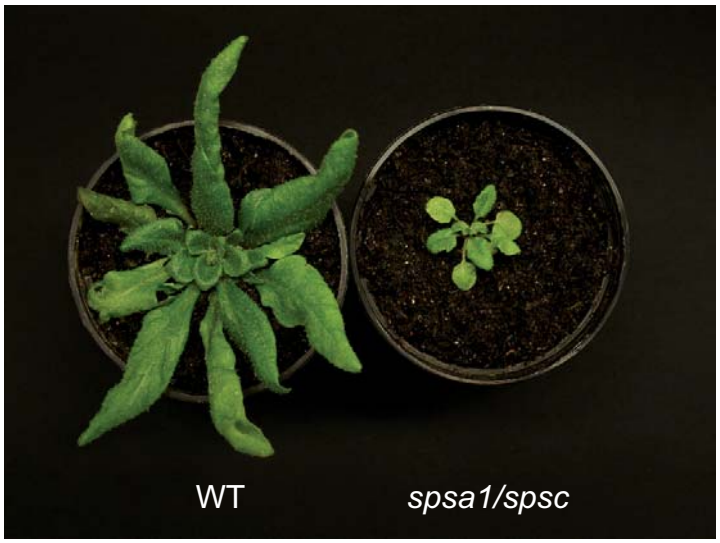
WT
spsa1/spsc

B

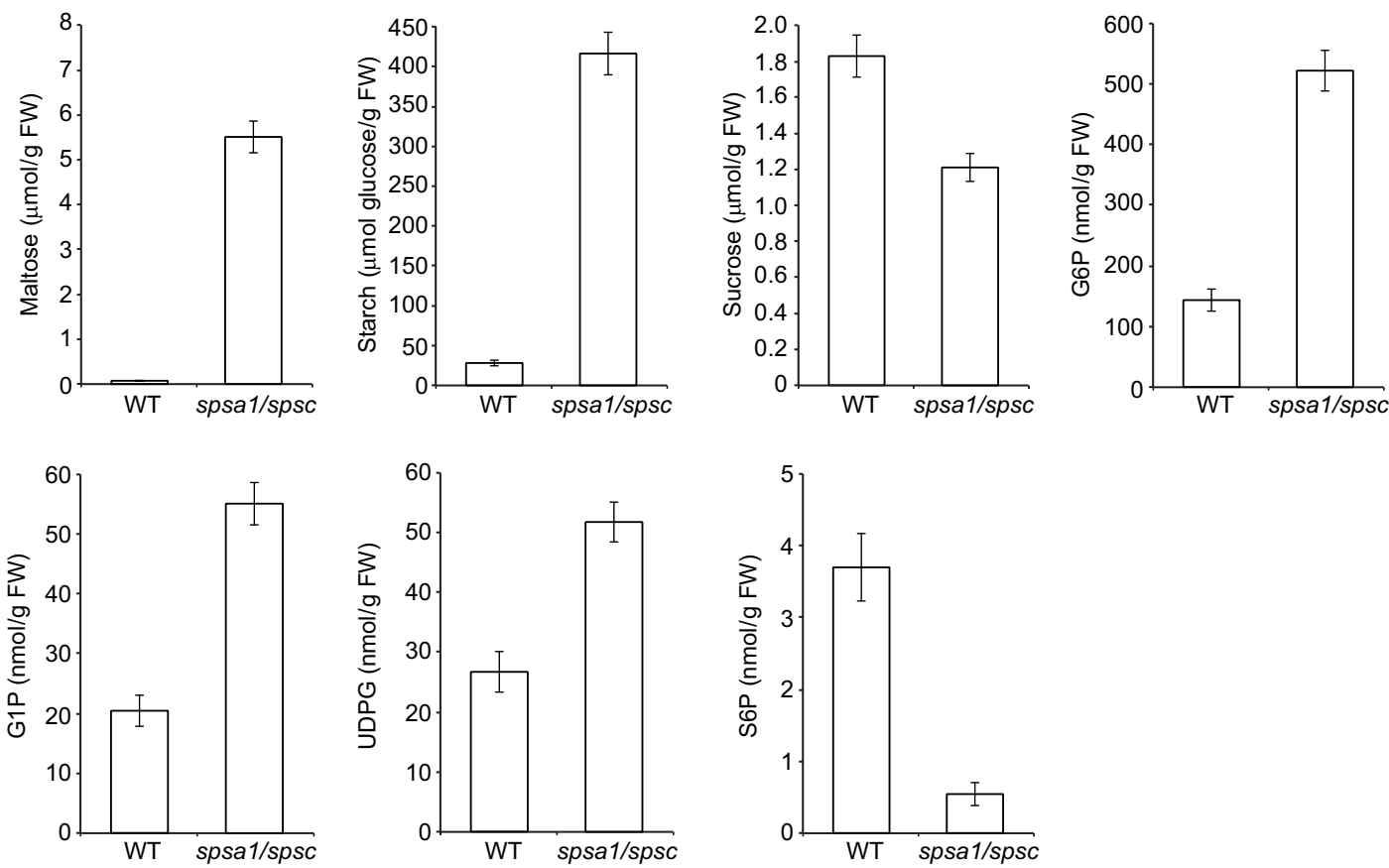
Maltose (µmol/g FW)
Starch (µmol glucose/g FW)
Sucrose (µmol/g FW)
G6P (nmol/g FW)
G1P (nmol/g FW)
UDPG (nmol/g FW)
S6P (nmol/g FW)
WT
spsa1/spsc

Figure 6

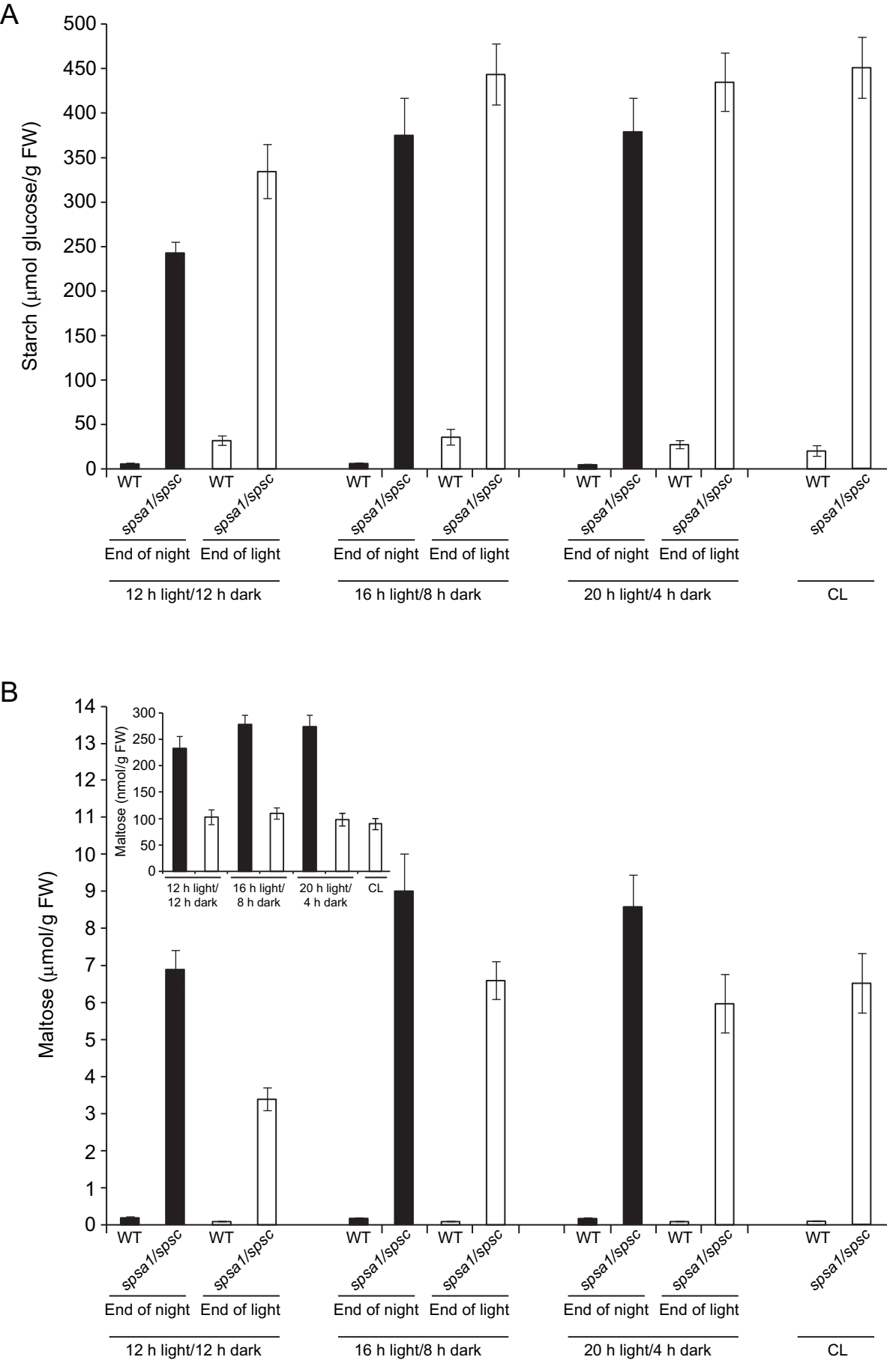
A
Starch (µmol glucose/g FW)
500
450
400
350
300
250
200
150
100
50
0
WT
spsa1/spsc
End of night
End of light
12 h light/12 h dark
16 h light/8 h dark
20 h light/4 h dark
CL
B
Maltose (µmol/g FW)
Maltose (nmol/g FW)
12 h light/ 12 h dark
16 h light/ 8 h dark
20 h light/ 4 h dark

Figure 7

Table S1: *sps* mutants used in this work and their phenotypes

Designation	Description	Source	Rosette Growth	Flower and silique growth, and seed production	Nonstructural carbohydrate content
spsa1/spsa2	*spsa1* and *spsa2* double mutant	This work	Like WT	Like WT	Like WT
spsa1/spsb	*spsa1* and *spsb* double mutant	This work	Like WT	Like WT	Like WT
spsa1/spsc	*spsa1* and *spsc* double mutant	This work	Reduced	Reduced	-High levels of UDPG, G1P, glucose and G6P, and very high levels of maltose and starch in plants cultured under different photoperiod conditions. -Low levels of sucrose and S6P. -High levels of OPPP, glycolytic and TCA intermediates and enzymatic activities.
spsa2/spsb	*spsa2* and *spsb* double mutant	This work	Like WT	Like WT	Like WT
spsa2/spsc	*spsa2* and *spsc* double mutant	This work	Like WT	Like WT	Like WT
spsb/spsc	*spsb* and *spsc* double mutant	This work	Like WT	Like WT	Like WT
spsa1/spsb/spsc	*spsa1*, *spsb* and *spsc* triple mutant	This work	Aberrant	Sterile	_
spsa1/spsa2/spsb	*spsa1*, *spsa2* and *spsb* triple mutant	This work	Like WT	Like WT	Like WT
spsa1/spsa2/spsc	*spsa1*, *spsa2* and *spsc* triple mutant	This work	Reduced	Reduced	Comparable to *spsa1/spsc*
spsa2/spsb/spsc	*spsa2*, *spsb* and *spsc* triple mutant	This work	Like WT	Like WT	Like WT
spsa1/spsa2/spsb/spsc	*spsa1*, *spsa2*, *spsb* and *spsc* quadruple mutant	This work	Aberrant	Sterile	_

Table S2. Primers used for PCR screening of *sps* mutants. For further details about annealing positions of RP, LP and T-DNA specific primers and PCR analyses of *sps* mutants, see **Fig. S2** and **Fig. S3**.

Mutant	**Primer**	**Sequence**
spsa1 (SALK_ 119162)	RP (*SPSA1*)	5'-aggaaaaagaagcacagaggc-3'
	LP (*SPSA1*)	5'-accagcatcagcatagtgtcc-3'
	LBb1 (T-DNA)	5'-gcgtggaccgcttgctgcaact-3'
spsa2 (SALK_ 064922)	RP (*SPSA2*)	5'-ccagctactctgaaccgtctg-3'
	LP (*SPSA2*)	5'-tgcaagacttacaaggttcgc-3'
	LBb1 (T-DNA)	5'-gcgtggaccgcttgctgcaact-3'
spsb (GABI_368F01)	RP (*SPSB*)	5'-ttgctatgacaatgagggagc-3'
	LP (*SPSB*)	5'-ttaaccggtgaatcaaccttg-3'
	Gabi (T-DNA)	5'-cccatttggacgtgaatgtagacac-3'
spsc (SAIL_31_H05)	RP (*SPSC*)	5'-ttttcaatatgctcgtgggac-3'
	LP (*SPSC*)	5'-gcgggaaaggacttataccac-3'
	LB3 (T-DNA)	5'-tagcatctgaatttcataaccaatctcgatacac-3'

Table S3. Primers used in RT-PCR analyses

Gene	**Direction**	**Sequence**
18S RNA At3g41768	Forward	5´-gggcattcgtatttcatagtcagag-3´
	Reverse	5´-cggttcttgattaatgaaaacatcct-3´
SPSA1 At5g20280	Forward	5´-aggaaaaagaagcacagaggc-3´
	Reverse	5´-accagcatcagcatagtgtcc-3´
SPSA2 At5g11110	Forward	5´-ccagctactctgaaccgtctg-3´
	Reverse	5´-caatgtaaggttcgcaagctc-3´
SPSB At1g04920	Forward	5´-ttgctatgacaatgagggagc-3´
	Reverse	5´-ttaaccggtgaatcaaccttg-3´
SPSC At4g10120	Forward	5´-gatgataaatcaagtcgaaacc -3´
	Reverse	5´-cattcgtggcatgtatctacc-3´

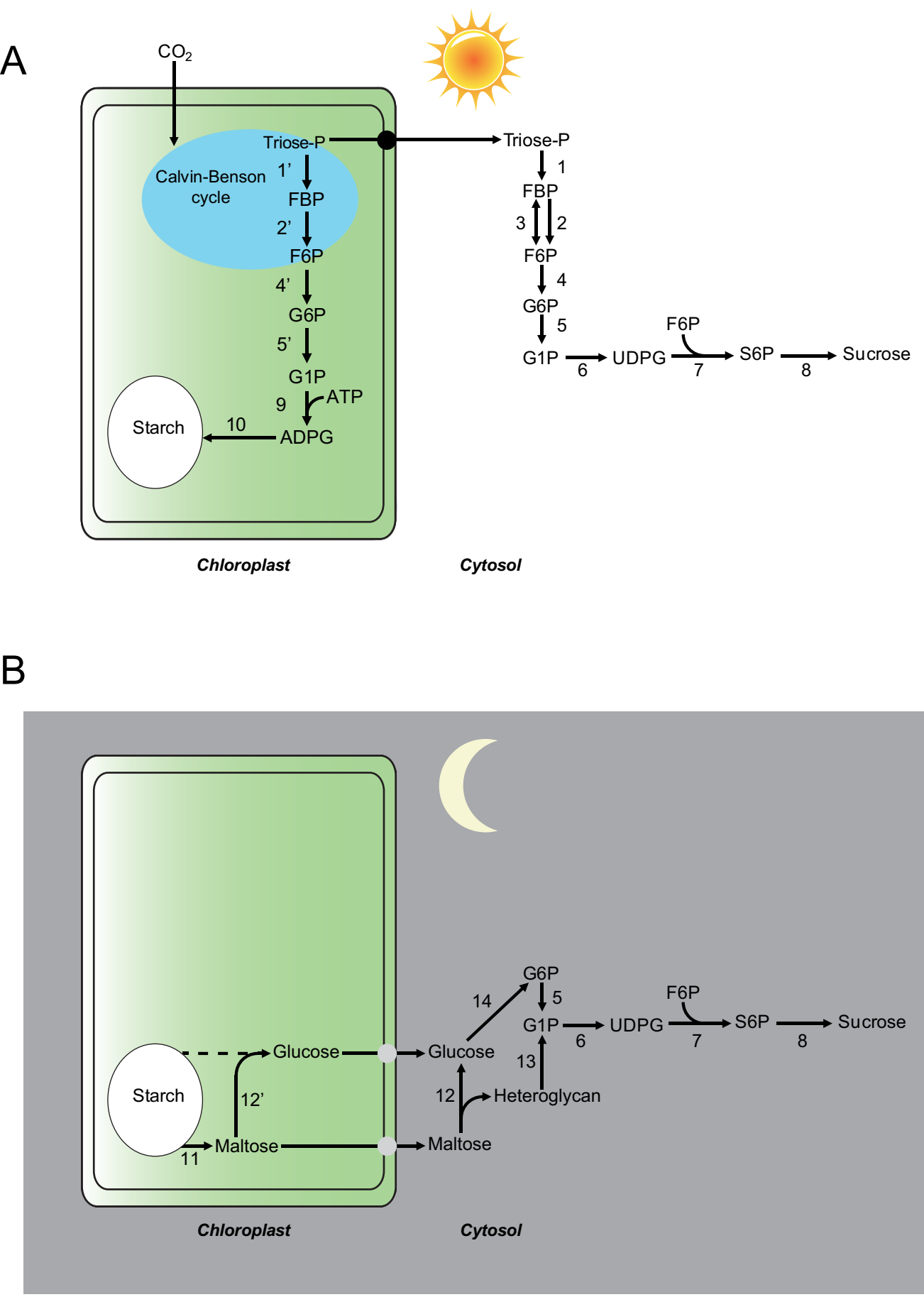

Supplemental Figure 1

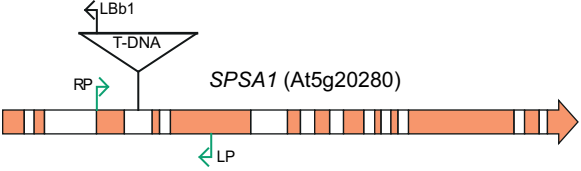

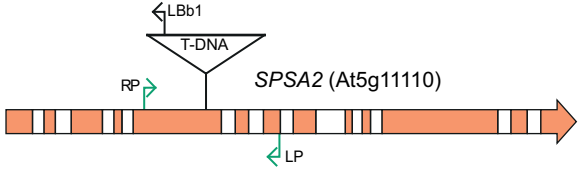

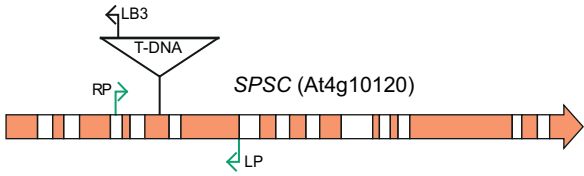

Supplemental Figure 2

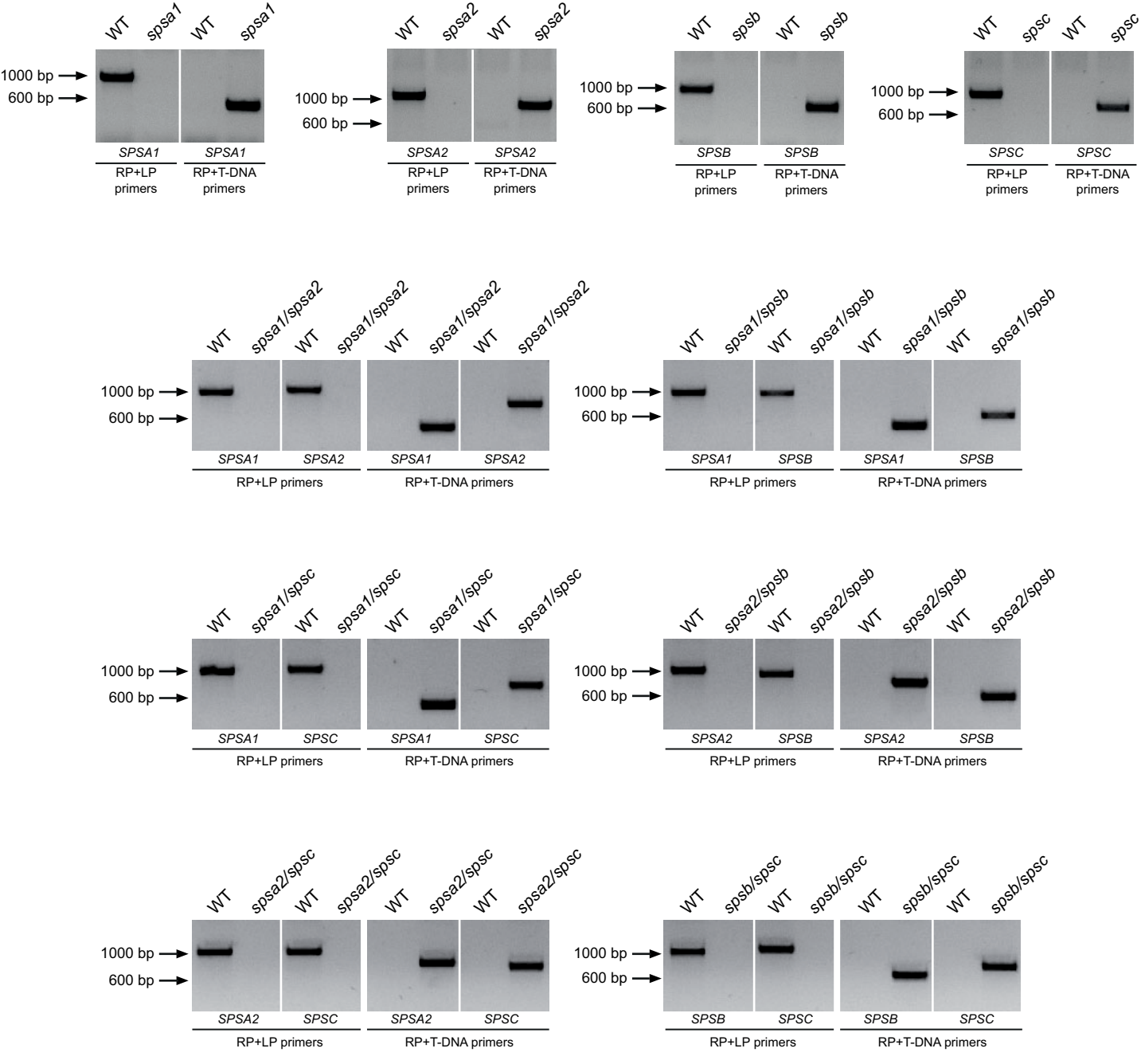

Supplemental Figure 3

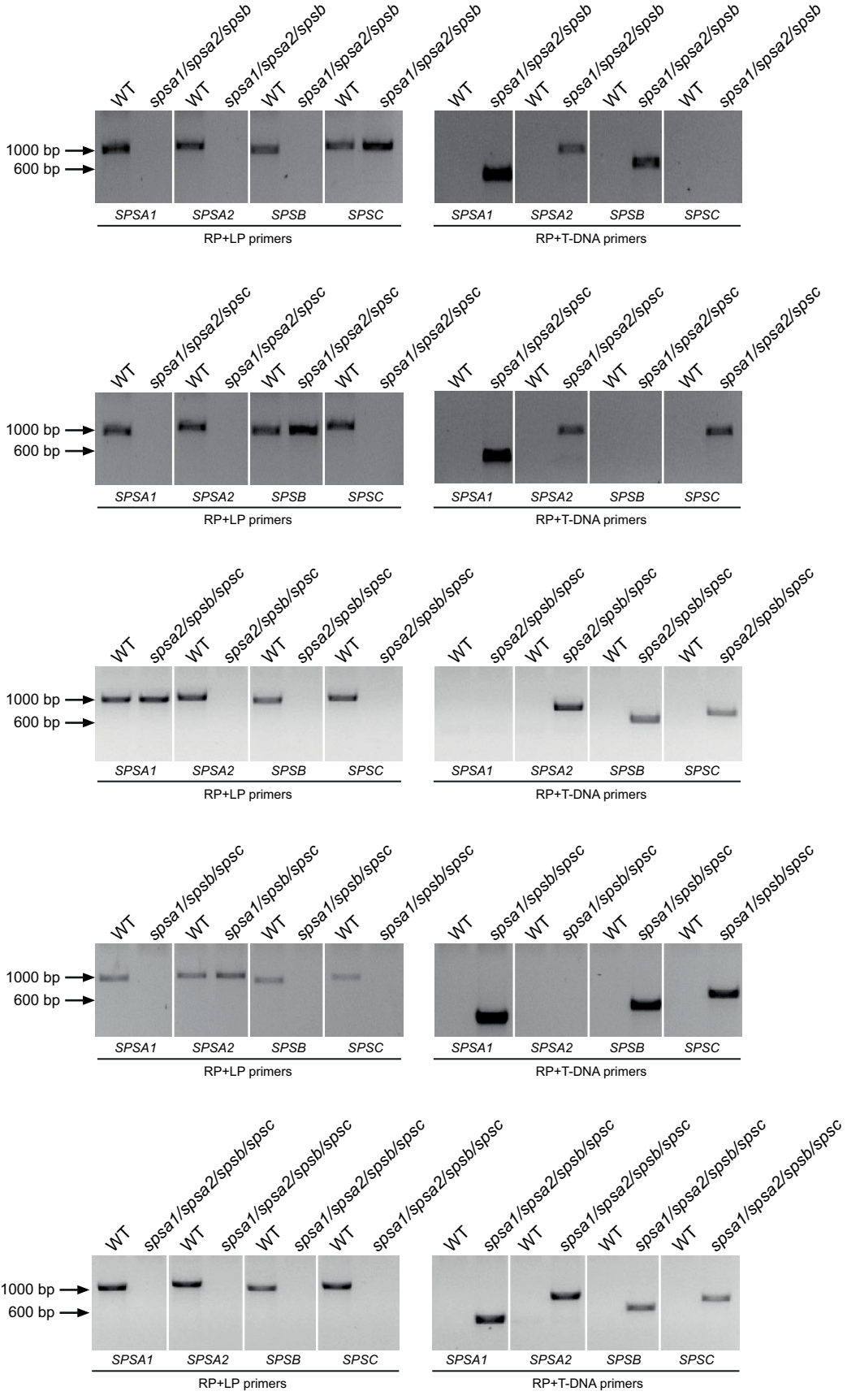

Supplemental Figure 3

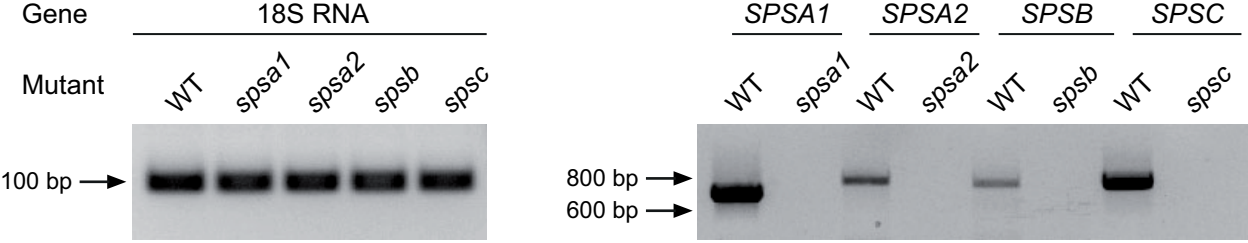

Supplemental Figure 4

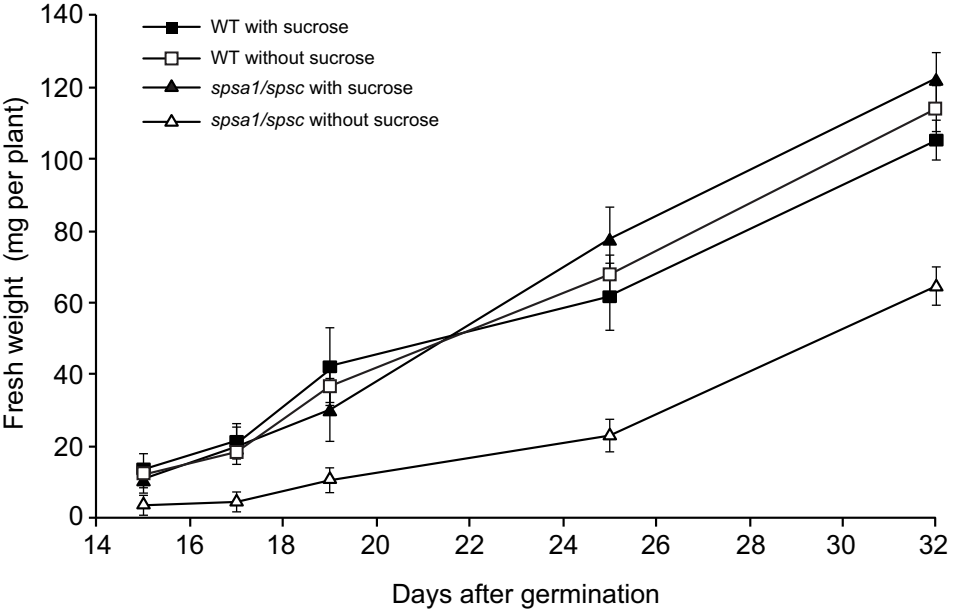

Supplemental Figure 5

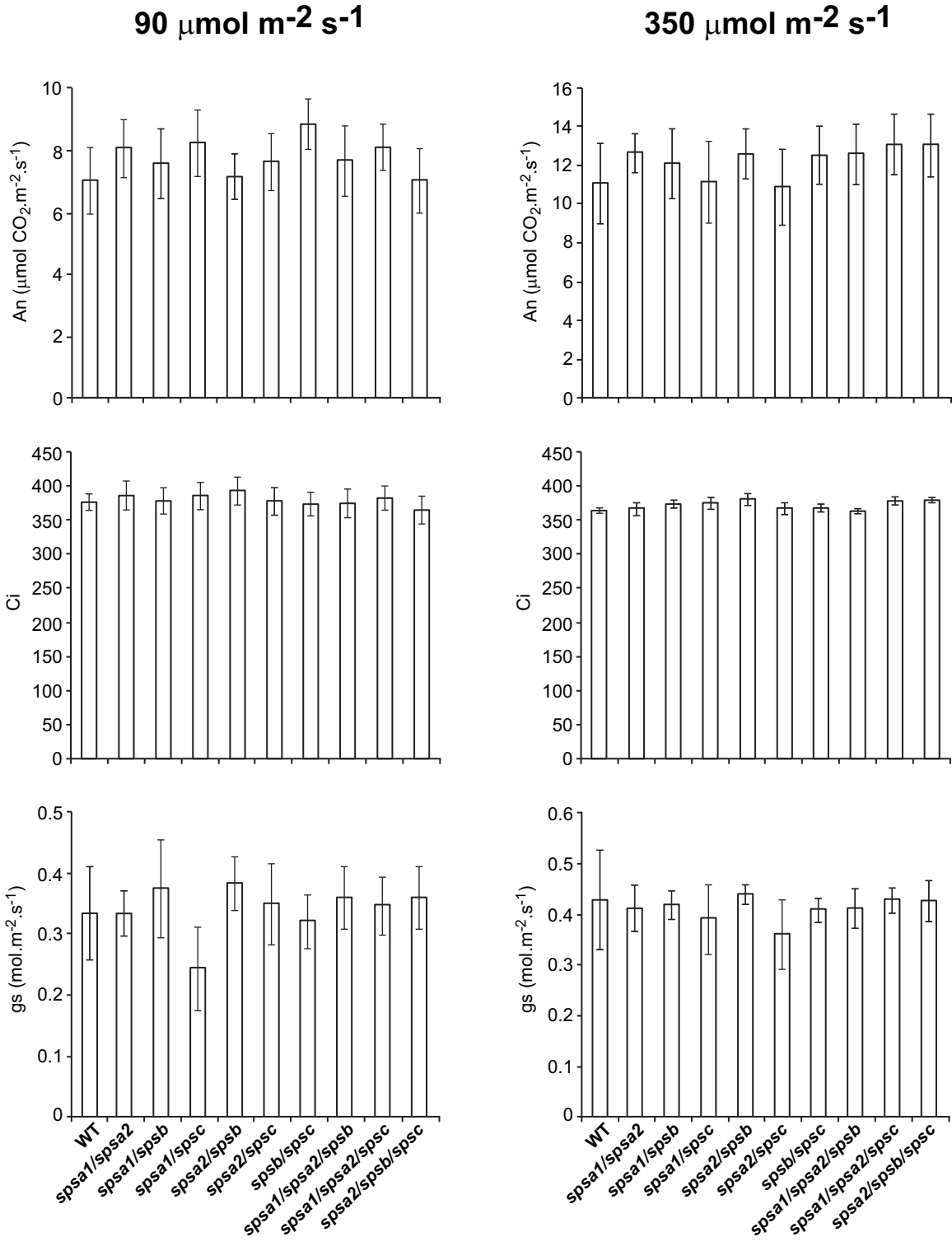

Supplemental Figure 6

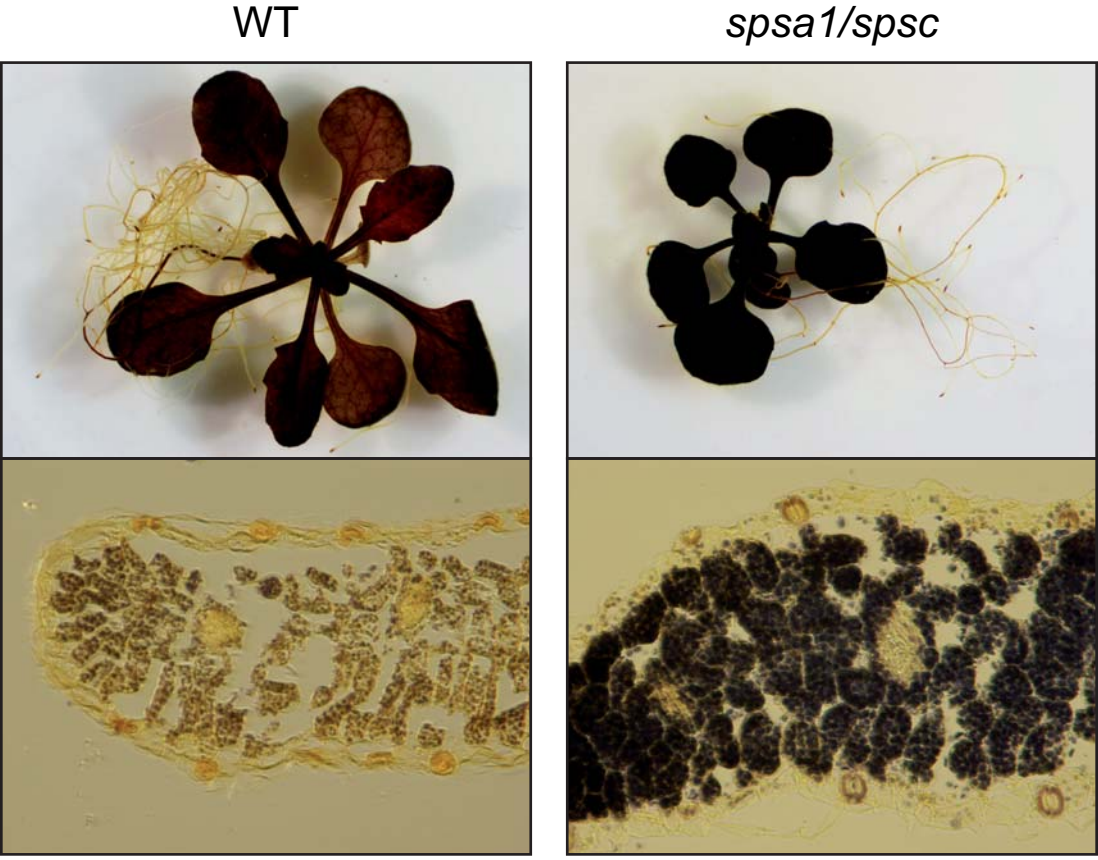

Supplemental Figure 7

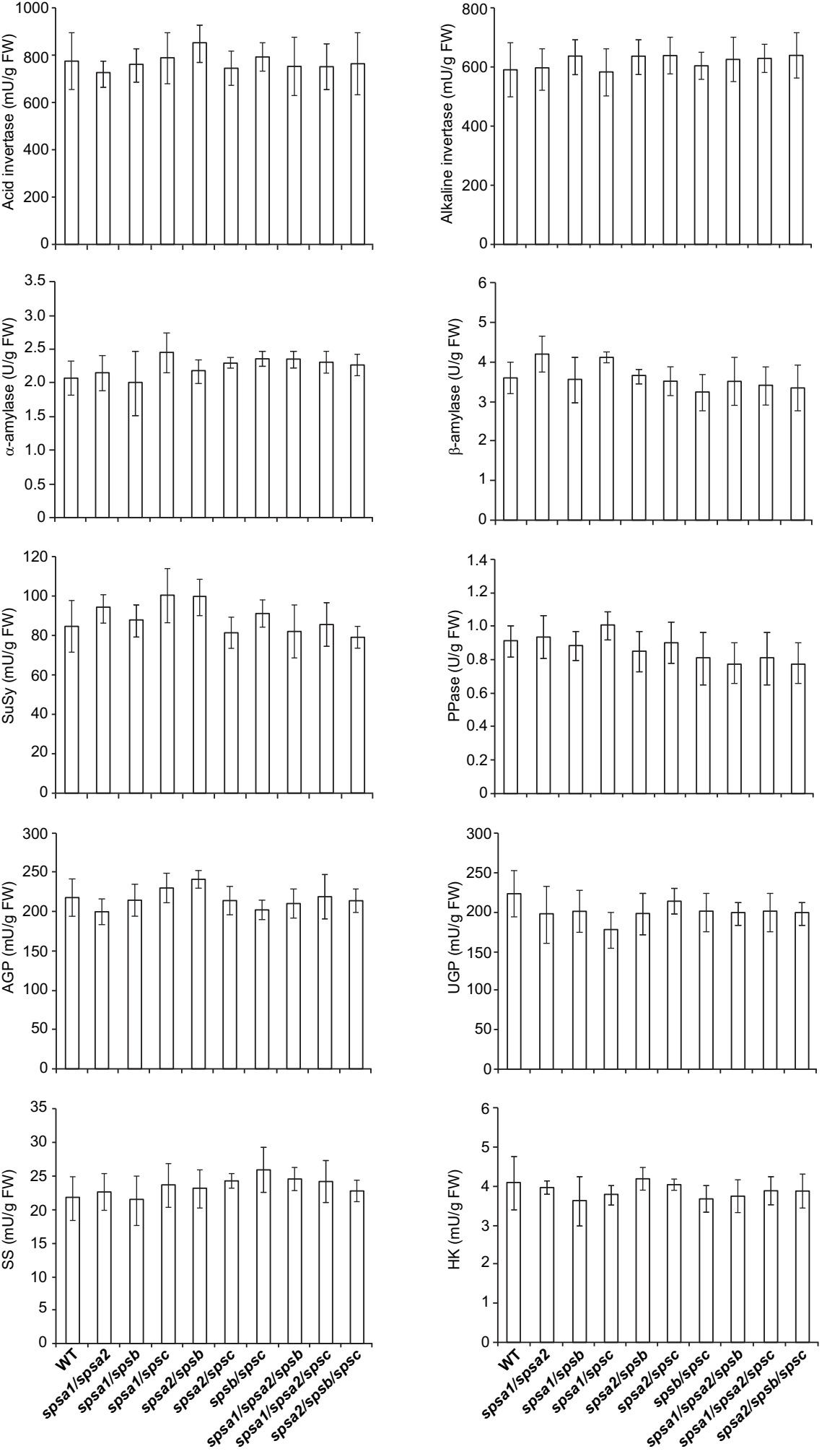

Supplemental Figure 8

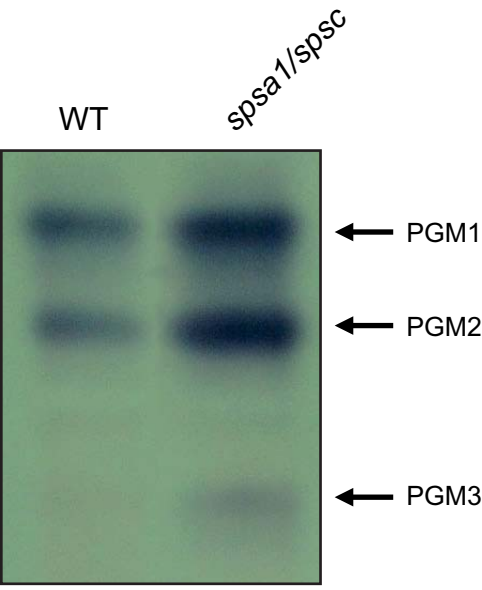

Supplemental Figure 9

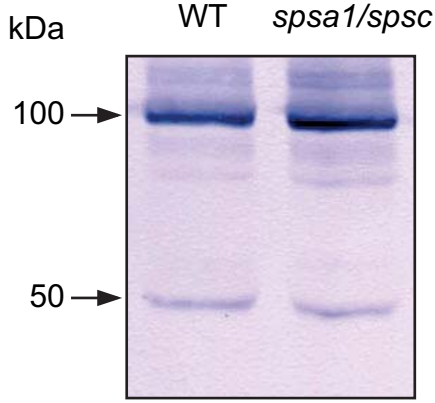

Supplemental Figure 10

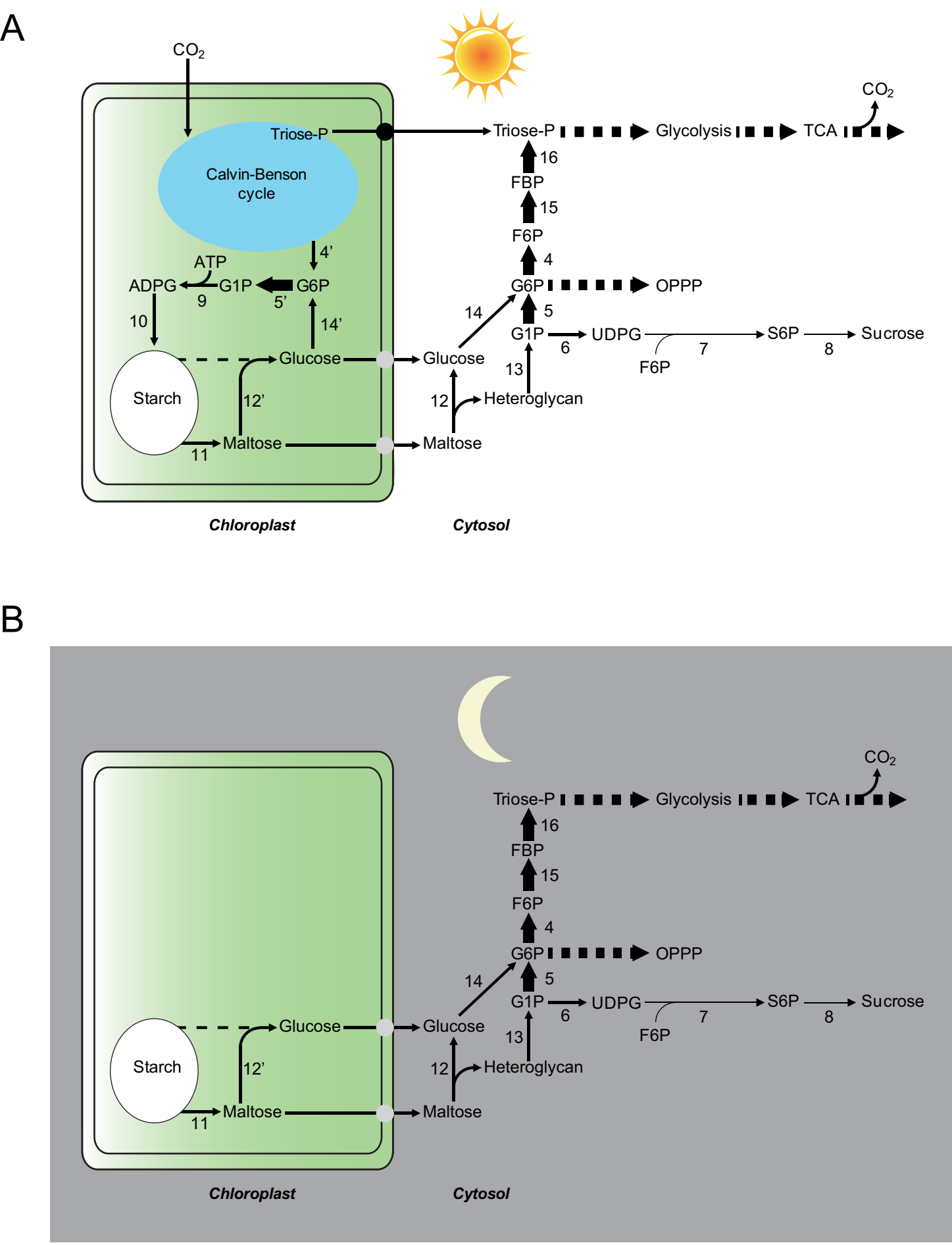

Supplemental Figure 11